

***Emiliana huxleyi* biometry and calcification response to the Indian Sector of the Southern Ocean environmental gradients**

Shramik M. Patil¹, Rahul Mohan^{1*}, Suhas S. Shetye², Vailancy Vaz¹, Sahina Gazi¹, Pallavi P. Choudhari, Syed A. Jafar³

¹ESSO-National Centre for Polar and Ocean Research, MoES, Vasco-da-Gama, Goa, India-403804

*shramikpatil@gmail.com, +91-(832) 2525531, fax- +91-(832) 2520877

²National Institute of Oceanography, Dona Paula, Goa, India-403004

³Flat 5-B, Whispering Meadows, Haralur Road, Bangalore- 560 102, India

Author emails: Shramik M. Patil: shramikpatil@gmail.com

Rahul Mohan: rahulmohan@ncpor.res.in

Suhas S. Shetye: suhasshetye@gmail.com

Vailancy Vaz: vailancyvaz29@gmail.com

Sahina Gazi: sahina2gazi@gmail.com

Pallavi P. Choudhari: pallavichoudhari20@gmail.com

Syed A. Jafar: syeda_jafar@yahoo.com

Abstract

An increase in the atmospheric $p\text{CO}_2$ and temperature is expected to reduce ocean CO_3^{2-} concentration, make oceans warmer and alter ocean circulation patterns. This will also affect the production and biogeographic distribution of marine calcifying organisms including coccolithophores. The lowering of oceanic CO_3^{2-} is expected to alter the coccolithophore calcification process and promote malformation of coccoliths, whereas changes in the oceanic temperature and circulation patterns may shift their biogeographic boundaries. In this study, we have investigated *Emiliana huxleyi* coccolith and coccosphere size response to the wide-ranging physico-chemical conditions of the Indian sector of the Southern Ocean between latitudes 38°S and 58°S during the austral summer of 2010 (January-February). This study helps to understand the response of *E. huxleyi* coccolith/coccosphere morphometry and mass changes to the fluctuating temperature, salinity, CO_3^{2-} , $p\text{CO}_2$, and nutrient values. Our results show that in the Indian sector of the Southern Ocean, *E. huxleyi* coccoliths are larger and coccospheres are smaller in the Subtropical Zone (STZ) whereas coccoliths size is smaller and coccospheres size is larger in the Subantarctic Zone (SAZ), which is due to the decrease in SST, SSS and increase in nutrient concentrations. In the Indian sector of the Southern Ocean, *Emiliana huxleyi* shows north to south morphotype shift from the heavily calcified 'Group A' (*E. huxleyi* morphotype A) to weakly calcified 'Group B' (*E. huxleyi* morphotypes B/C, C) forms. We demonstrate that although weakly calcified *E. huxleyi* morphotypes (morphotypes B/C and C) coccoliths comprise less mass than that of the *E. huxleyi* morphotype A coccoliths, due to the large-sized coccospheres and numerous coccoliths per coccosphere, 'Group B' coccospheres precipitate large amount of CaCO_3 in the SAZ compared to 'Group A' coccospheres located in the STZ. In addition, we documented the presence of large *E. huxleyi* overcalcified coccospheres with large sized coccoliths in the southernmost cold, high $p\text{CO}_2$, and nutrient-rich waters which show extracellular calcite precipitation. The energy dispersive spectrometry analysis indicates the presence of a large amount of Mg in the overcalcified *E. huxleyi* specimens. We suspect that the *Emiliana huxleyi* in the colder nutrient-rich waters, with predicted changes in the carbonate chemistry, may adapt to low pH, high $p\text{CO}_2$ conditions through extracellular Ca and Mg mineralization.

Keywords: Coccolithophores, Overcalcification, Magnesium, Carbonate chemistry, $p\text{CO}_2$

1. Introduction

The anthropogenic carbon dioxide (CO₂) emission since the Industrial Revolution has lowered the surface ocean pH by ~0.1 units, a process well known as the ocean acidification (Caldeira and Wickett, 2003). If these CO₂ emissions continue to occur at the current pace, the ocean pH is expected to drop by another 0.06-0.32 units by the end of 2100 (IPCC, 2019). This decrease in the ocean pH will reduce the calcium carbonate (CaCO₃) saturation state by 2.0 units (Kleypas et al., 1999) and affect the production and calcification of marine calcifying organisms including coccolithophores (Zondervan et al., 2002; Feely et al., 2004; Engel et al., 2005; Beaufort et al., 2011). Recent ocean-carbon cycle models indicate that the polar and subpolar ecosystems are the first to be affected by increasing CO₂ emissions and are near undersaturation with respect to CaCO₃ minerals in the upcoming decades (Feely et al., 2009). In particular, the colder temperatures and mild alkalinity of the Southern Ocean make it highly vulnerable to future warming and acidification (Cao and Caldeira, 2008; Shadwick et al., 2015), thereby affecting marine calcifying organisms especially coccolithophores which are abundant in the Southern Ocean (Balch et al., 2011, 2016; Patil et al., 2017, 2020).

In general, coccolithophores form a significant component of the marine phytoplankton community which ranges from the tropical to the high latitude regions (Jordan and Chamberlain, 1997; Paasche, 2002) and often forms prolific blooms extending hundreds to thousands of kilometers. Among the known coccolithophores, *Emiliania huxleyi* is the most abundant and ubiquitous coccolithophore which often forms blooms in a wide range of environments (i.e. tropical to Polar Regions and neritic to oceanic waters (Tyrell and Young, 2009; Rigual-Hernández et al., 2020)) and comprise larger abundances in the southern high latitude regions (Balch et al., 2011; Rigual-Hernández et al., 2020). It is estimated that annually, *E. huxleyi* blooms cover ~1x10⁶ km² areal extent equivalent to ~0.28% of the global ocean (Brown and Yoder, 1994; Rigual-Hernández et al., 2020) with concentrations reaching up to 10⁸ cells L⁻¹. In the Southern Ocean, high abundances of *E. huxleyi* contribute for the circum-global Great Calcite Belt (GCB) that covers >60% of the Southern Ocean and is characterized by PIC concentrations ~1 μmol.L⁻¹ compared to the global average of 0.2 μmol.L⁻¹ (Balch et al., 2011). Owing to such high abundance, *E. huxleyi* plays a significant role in the marine carbon cycle thereby influencing ocean-atmospheric CO₂ exchange and export of inorganic and organic carbon to the deeper oceanic depths (Klaas and Archer, 2002). Understanding the importance of coccolithophores in the global climate, several studies explaining the possible future response of coccolithophores (and other calcifying organisms) to change in CO₃²⁻ chemistry, and warming has

been attempted in laboratory-controlled as well as in-situ experiments which could give rise to inconsistent interpretations.

Most of the laboratory controlled seawater acidification experiments resulted in the reduced calcification rates in planktonic foraminifera (Bijma et al., 2002), cold-water corals (Fabry et al., 2009), and pteropods (Manno et al., 2017). However, laboratory-controlled experiments on *E. huxleyi* indicate a varying response of coccolithophore calcification, reporting decreased (Riebesell et al., 2000; Zondervan et al., 2002), increased (Iglesias-Rodriguez et al., 2008; Fiorini et al., 2011) or unchanged (Richier et al., 2011; Jones et al., 2013) calcification with decreasing CO_3^{2-} concentrations. Multiple factors have been presumed to be responsible for varying calcification response including differences in the methodology protocols, and strain-specific calcification response to pH change (Riebesell et al., 2000; Iglesias-Rodriguez et al., 2008; Langer et al., 2009; Lohbeck et al., 2012; Müller et al., 2015). Though laboratory-controlled experiments provide important information on *E. huxleyi* physiological response, they cannot mimic natural environmental settings (e.g., minute changes in the temperature, salinity, light intensity, stratification, and macro- and micronutrient concentrations) which usually have crucial control over coccolithophore production, calcification, and spatial distribution (Perrin et al., 2016; Matson et al., 2016; Feng et al., 2008). Therefore, field experiments are essential to validate laboratory observations (e.g., Trinantaphyllou et al., 2018) and relate the laboratory-controlled experiments results to the natural field environment. In-situ coccolith size measurements in the widely fluctuating environmental conditions (e.g., Southern Ocean) provide a valuable approach to assess the response of coccolithophore/coccolith size and calcification to the environmental changes (including changes in nutrients, temperature, salinity, pCO_2 , and CO_3^{2-} concentration). The studies on mixed *E. huxleyi* populations provide a combined response of *E. huxleyi* taxa to the vital environmental and oceanographic changes which has benefit over strain specific laboratory controlled experiments. The field-based observations can be a reliable tool to study the effect of seasonality on *E. huxleyi* coccolith/coccosphere size and to document morphometric differences within the morphotypes in the changing environmental conditions. The coccolith/coccosphere size-based information potentially be used to back-calculate the coccolithophore production in the surface waters, sediment traps, and paleo investigations.

Keeping this in view, we carried out *E. huxleyi* morphometric measurements in the samples collected between the Subtropical Zone and the Antarctic Zone of the Indian sector of the Southern Ocean. We measured several morphometric parameters of *E. huxleyi* coccoliths and coccospheres to investigate:

- (1) Changes in *E. huxleyi* morphotypes coccolith and coccosphere size in response to the changing environmental conditions,
- (2) *E. huxleyi* morphotypes coccolith and coccosphere mass variation and CO_3^{2-} contribution in the Indian sector of the Southern Ocean, and
- (3) The possible response of *E. huxleyi* morphotypes production and distribution to future CO_3^{2-} , physico-chemical and environmental changes.

2. Background

2.1 Oceanographic settings

This study was conducted in the Indian sector of the Southern Ocean between Mauritius and Antarctica during the austral summer of 2010 (January-February). In the Indian sector of the Southern Ocean, major oceanic fronts and frontal zones recognized in the poleward direction are, the Agulhas Retroflection Frontal Zone (ARFZ), the Agulhas Retroflection Front (ARF), the Subtropical Zone (STZ), the Southern Subtropical Front (SSTF), the Subantarctic Zone (SAZ), the Subantarctic Front (SAF), the Polar Frontal Zone (PFZ), the Polar Front (PF), the Antarctic Zone (AZ), and the Antarctic Divergence (AD) (Orsi et al., 1995) (Fig. 1). In the Indian sector of the Southern Ocean, the oceanic fronts split, merge, fluctuate seasonally, and vary spatially over the topographic features (Anilkumar et al., 2006). In this region, during the austral summer, elevated biological activity is documented in the frontal zones with increased upwelling activity. Between the STZ and AZ, chlorophyll-a concentration ranges between 0.1 mg/m^3 and 0.64 mg/m^3 , with the highest values at the SAZ and PFZ and lowest at the STZ and AZ (Shetye et al., 2015). Whereas, primary productivity values range from $185 \text{ mg C m}^{-2} \text{ d}^{-1}$ to $>900 \text{ mg C m}^{-2} \text{ d}^{-1}$ (Gandhi et al., 2012), with typically high productivity at the SSTF ($>900 \text{ mg C m}^{-2} \text{ d}^{-1}$) and low productivity at the AZ ($\sim 185 \text{ mg C m}^{-2} \text{ d}^{-1}$).

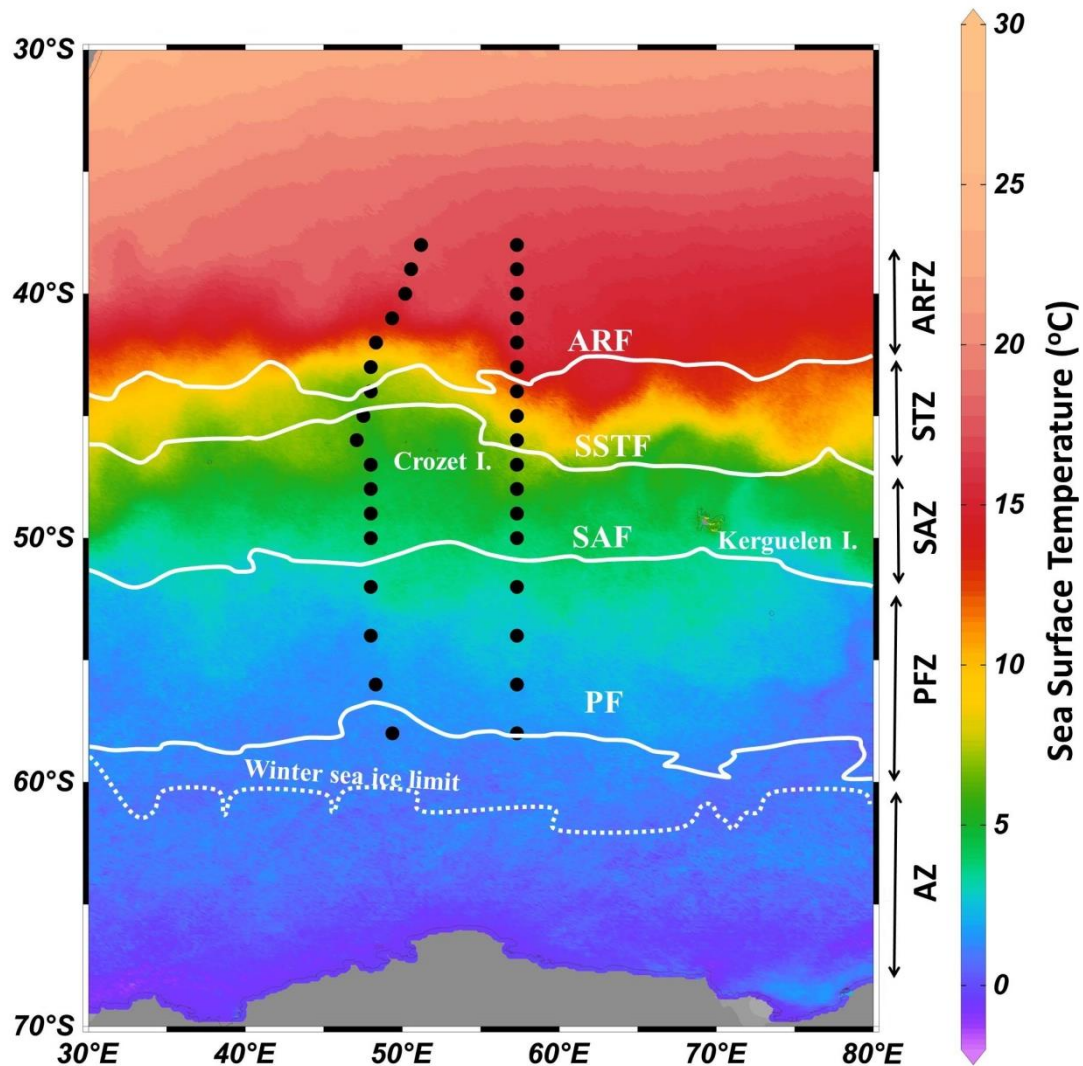


Fig 1. Location of the surface water samples used in this study. [Annotations: ARFZ- the Agulhas Retroflexion Frontal Zone; ARF- the Agulhas Retroflexion Front; STZ- the Subtropical Zone; SSTF- the Southern Subtropical Front; SAZ- the Subantarctic Zone; SAF- the Subantarctic Front; PFZ- the Polar Frontal Zone; PF- the Polar Front; AZ- the Antarctic Zone]. [In the fig. color patterns indicate monthly averaged sea surface temperature data (January-February 2010) obtained from giovanni.gsfc.nasa.gov).

2.2 *Emiliana huxleyi* morphotypes differentiation

In the field-based investigations, different *E. huxleyi* morphotypes were recognized based on the visual expression of the degrees of calcification (McIntyre and Bé, 1967; Young and Westbrook, 1991; Hagino et al., 2011; Patil et al., 2017) which potentially represent genetic varieties (Medlin et al., 1996). *Emiliana huxleyi* morphotypes differ in robustness/thickness of the distal shield elements, central area closure, and thickness of the tube which is interpreted as differences in the degree of calcite production. With the advances of field investigations in different oceanographic realms, more *E. huxleyi* variants were recognized and supported sub-dividing into two groups viz. ‘Group A’ and

‘Group B’ (Mikrotax.org). The ‘Group A’ comprises heavily calcified *E. huxleyi* morphotypes (viz. *E. huxleyi* morphotypes A, A overcalcified, R, and var. *corona*) which are easily distinguishable based on their robust distal shield elements, sub-parallel shields, highly variable tube width, and grill in the central area. On the contrary, ‘Group B’ *E. huxleyi* morphotypes (viz. *E. huxleyi* morphotypes B, B/C, C, and O) are differentiated based on the delicate distal shield elements, a curved distal shield which often smaller than the proximal shield, narrow tube, and open or closed central area. The sub-division of ‘Group B’ coccoliths is done mostly based on their size, but the coccolith size can vary geographically with differing response to the oceanographic settings. The central area in ‘Group B’ *E. huxleyi* morphotypes can be open or covered with a thin plate. The open central area occurs in most size ranges but in the smaller specimens, it is difficult to distinguish whether the central area is covered by a calcareous structure or organic membrane thus may need further culture-based observations. It is to be noted that culture-based investigations did not document changes in *E. huxleyi* morphology from ‘Group A’ to ‘Group B’ and vice versa (Linge Johnsen et al., 2020) eliminating chances of making morphologically different coccoliths by a single strain (www.mikrotax.org).

2.3 *Emiliania huxleyi* morphotypes distribution in the Southern Ocean

In the Southern Ocean, *E. huxleyi* contributes >70% to total coccolithophore production in the STZ-SAZ and over 90-100% in the PF regions (Saavedra-Pellitero et al., 2014; Patil et al., 2017; 2020). The *E. huxleyi* abundance declines south of the PF (Findlay and Giraudeau, 2000; Mohan et al., 2008; Saavedra-Pellitero et al., 2014; Patil et al., 2017; Rigual Hernández et al., 2018) but the occasional occurrence of *E. huxleyi* coccospheres and coccoliths are often documented in the Southern high latitudes in lower abundances (Patil et al., 2014; Winter et al., 1999). Overall, *E. huxleyi* populations in the Southern Ocean are primarily composed of morphotypes A, A overcalcified, R, B/C, C, O, and var. *corona* (*E. huxleyi* groups A and B) which show differences in the latitudinal distribution patterns (Malinverno et al., 2015; Patil et al., 2017; Saavedra-Pellitero et al., 2019).

In the Indian and Atlantic sectors of the Southern Ocean, *E. huxleyi* populations are dominated by morphotype C followed by morphotype B/C. Together, these two morphotypes comprise >80% of the total coccolithophore abundance (Cubillos et al., 2007; Saavedra-Pellitero et al., 2014; Patil et al., 2014, 2017; 2020) and show occurrence as far as the PF region. In the Indian and Atlantic sectors of the Southern Ocean, heavily calcified *E. huxleyi* morphotype A is geographically restricted to the warmer waters and indicates elevated abundances in the STZ and SAZ (Saavedra-Pellitero et al., 2014; Patil et al., 2017). The overcalcified *E. huxleyi* morphotype A specimens were rarely documented in the Atlantic sector (Saavedra-Pellitero et al., 2014) but are not observed in the Indian sector so far (Mohan et al., 2008; Patil et al., 2013, 2014, 2017; 2020).

On the contrary, in the Australian sector of the Southern Ocean, south of Tasmania, *E. huxleyi* populations are primarily composed of morphotypes A overcalcified, A, and B/C which show substantial seasonal variations in their absolute and relative abundances (Cook et al., 2011; Cook et al., 2013; Rigual-Hernández et al., 2020), however, this region is devoid of weakly calcified *E. huxleyi* morphotype C. In the Australian sector of the Southern Ocean, *E. huxleyi* morphotype A overcalcified specimens dominate at the north of the SAF and morphotype A dominates between the STF and the PF; whereas, *E. huxleyi* morphotype B/C specimens dominate from the SAF to as far as 65°S (Cubillos et al., 2007; Rigual Hernández et al., 2018). In the Australian sector, *E. huxleyi* morphotype B/C becomes the only morphotype that survives in the AZ waters (Rigual Hernández et al., 2018).

The recent investigations in the Drake Passage (Saavedra-Pellitero et al., 2019) showed the presence of heavily calcified ‘Group A’ *E. huxleyi* morphotypes i.e. *E. huxleyi* morphotype A and type R along the Chilean margin, ‘Group B’ *E. huxleyi* morphotypes i.e. *E. huxleyi* morphotypes B/C, C, and O in the SAZ, and *E. huxleyi* morphotypes B/C and C in the PFZ.

In the West Pacific sector of the Southern Ocean, *E. huxleyi* morphotype A is present in the northern SAZ, and type O and B/C dominates up to the PFZ (Malinverno et al., 2015). This study also documents slight overcalcification in *E. huxleyi* coccolithophores at few sites. Overall observations in the Indian, Atlantic, Australian and Pacific sectors of the Southern Ocean indicate a consistent poleward latitudinal succession from heavily calcified *E. huxleyi* ‘Group A’ to moderate-weakly calcified ‘Group B’.

The occurrence of *E. huxleyi* morphotypes and latitudinal extent of these groups may vary based on the oceanic regions and environmental and oceanographic settings. The high genomic variability and consequent physiological adaptation are a primary reason for *E. huxleyi* ecological success (Read et al., 2013). However, *E. huxleyi* clades are well separated as per definitions but are not always morphologically distinguishable (Read et al., 2013).

3. Materials and methods

3.1 Water sample collection

Thirty-four sea surface water samples were collected onboard ORV Sagar Nidhi between 38°S and 58°S using a Niskin sampler and transferred into a clean prewashed plastic bottle for biological and chemical analysis. One to two-liter water was filtered onto 47mm diameter Nucleopore track-etched membrane filters with 0.8µm diameter pore size under low vacuum. Without any chemical treatment, rinsing, or washing, filter papers were shifted into plastic sterile petri dish, oven/air-dried at 40°C for 24 hours, and kept sealed until Scanning Electron Microscope (SEM) analysis. Surface water

samples collected between 38°S and 58°S during January-February 2010 were chosen based on *E. huxleyi* densities from Patil et al. (2020) for this study (Fig. 1). The samples located south of 58°S consists of low *E. huxleyi* abundance/devoid of coccolithophores hence were omitted from the analysis. The details of sampling locations and in-situ environmental parameters are provided in table 1.

3.2 SEM analysis

A rectangular piece of filter paper was cut from each filter, mounted on a double-sided carbon tape attached on a 1cm diameter aluminum stub, and sputter-coated with platinum using a JEOL JFC-1600 Auto Fine Coater. At least 125 *E. huxleyi* coccoliths and 50 *E. huxleyi* coccospheres per sample were manually captured at 20000x-25000x and 6000x-7000x magnification respectively using a JEOL JSM 6360 LV SEM (JEOL Japan). *Emiliania huxleyi* coccoliths and coccospheres were counted and classified into various morphotypes and/or morphological groups. At least 25 coccoliths and 10 coccospheres of each *E. huxleyi* morphotypes were measured in every sample, wherever possible (for instance, *E. huxleyi* morphotype A is not documented in the PFZ). The classification of *E. huxleyi* morphotypes A, B/C, and C were carried out following definitions of Young et al. (2003), (Mikrotax.org), and previously published literature from the Southern Ocean (e.g., Cubilos et al., 2007; Mohan et al., 2008; Boeckel and Baumann, 2008; Malinverno et al., 2015; Saavedra-Pellitero et al., 2014, 2019). Coccoliths with distal shield irregularly formed, missing central tube, and disconnected distal shield elements were recognized as malformed and avoided from morphometric measurements.

3.3 Elemental analysis

Energy Dispersive Spectrometry (EDS) was carried out on regular *E. huxleyi* and overcalcified *E. huxleyi* forms to assess their elemental composition. For EDS analysis, real-time images were captured by Oxford Aztec software, and point analysis per spectrum was carried out using 15KV accelerating voltage and up to 70,000× magnification. A total of 20 *E. huxleyi* coccospheres were analyzed to evaluate Mg and Ca concentrations.

3.4 Coccolith and coccosphere measurements

The coccoliths measurements [viz. Length of the Distal shield (DL), Width of the Distal shield (DW), Length of the Central area (CL), Width of the Central area (CW), Tube thickness (T), Total coccolith Area (TA), coccolith Central Area (CA)] (Fig. 2a) and coccosphere measurements [number of coccoliths per coccosphere (following Boeckel and Baumann, 2008), Area of coccosphere] (Fig. 2b) were carried out using Fiji/ImageJ 1.52d software (nannotax.org) and Coccobiom2 macros (www.tmsoc.org). Corroded/broken coccoliths were avoided for measurement since the morphometric measurements cannot be accurately determined. Since coccoliths on a coccosphere are not always

possible to measure without errors, coccoliths belong to a single broken coccosphere (fallen/spread at one place) were used. To do so, over 5000 fields of views at 3000x magnification were scanned and images were captured.

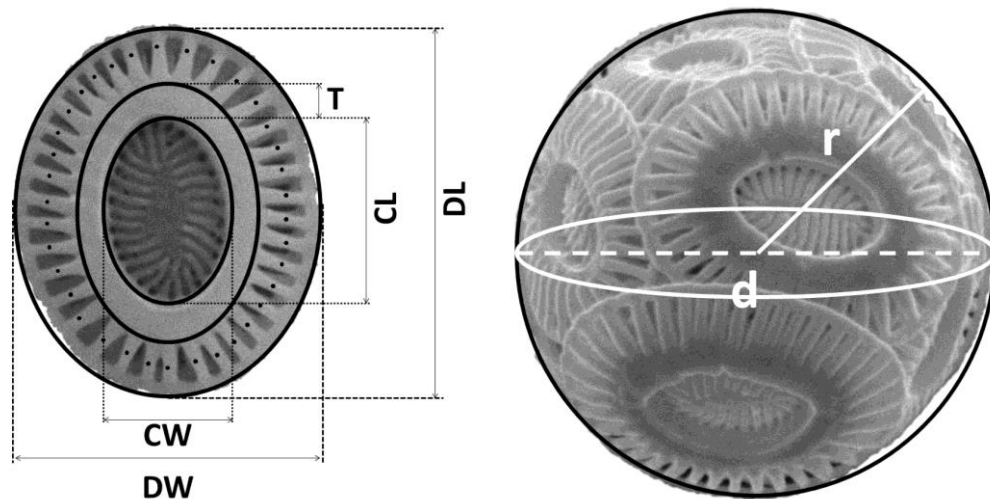


Fig. 2. Measurements were carried out on (a) *Emiliana huxleyi* coccoliths and (b) coccospheres digitized using Scanning Electron Microscope. [Annotations: DL=length of the distal shield; DW= width of the distal shield; CL= length of the central area; CW= width of the central area; T= tube thickness; r=radius; d=diameter]. Area of coccosphere= $4\pi r^2$.

3.5 Coccolith and coccosphere mass

Emiliana huxleyi morphotypes coccolith mass calculation followed after Young and Ziveri (2000). The method relies on a systematic relation between length and thickness of the coccolith and the calcite content of the given coccolith.

Coccolith mass calculation was carried out using a formula,

$$\text{Coccolith calcite mass (pg)} = 2.7 \times k_s \times l^3 \dots\dots (1)$$

Where 2.7 is the density of calcite ($\text{pg}/\mu\text{m}^3$), k_s is a shape constant for coccolith morphotypes, and l is the coccolith distal shield length in microns. Shape factors (k_s) for different morphotypes were obtained from literature estimates and are as follows: *E huxleyi* type A - 0.02 (Young and Ziveri, 2000; Poulton et al., 2010; Poulton et al., 2011) *E huxleyi* type B/C - 0.015 (Poulton et al., 2011; Holligan et al., 2010 and Charalampopoulou et al., 2016). *Emiliana huxleyi* type C k_s factor is not available hence the lowest shape factor value (0.015) available is considered. For length, an average value of ~20-50 coccoliths distal shield length for each morphotypes from this study area (48°E and 57.3°E) is used.

3.6 Environmental data

The Sea Surface Temperature (SST) was recorded using a bucket thermometer (accuracy: $\pm 0.2^\circ\text{C}$), Sea Surface Salinity (SSS) was computed using conductivity which was measured by Autosal model No-8400A. Nutrient Analysis [nitrate (NO_3), nitrite (NO_2), phosphate (PO_4), and silicate (SiO_4)] was carried out on-board using Shimadzu UV-1800 spectrophotometer following standard protocols of Grasshoff (1983). pCO_2 and CO_3^{2-} was calculated using TCO_2 (total CO_2) and pH in Total Scale (pH_T). The nutrient data for both the studied transects were published previously by Shetye et al., 2015. However, in the present study, nutrient data has been added in the figs. 3, 4, and table 1 for reference.

3.7. Statistical analysis

To examine the relationship between *E. huxleyi* morphometrics and measured environmental parameters, two different analyses were performed viz. Canonical Correspondence Analysis (CCA), and correlation analysis.

The CCA performed on the *E. huxleyi* measurements as well as environmental variables using Multivariate Statistical Package Program (MVSP) (Kovach, 1998). This analysis helps us to understand the relationship between *E. huxleyi* coccolith and coccosphere morphology and in-situ environmental data. In the CCA plots, the physico-chemical parameters are plotted as arrows which show the direction of increasing values of environmental variables. The length of arrow is directly proportional to the importance of the environmental variables, whereas the angle between the ordination axis and arrow indicates the extent of correlation between them, viz. smaller the angle, the stronger is the correlation. A perpendicular line drawn from the arrow through coccolithophore species indicates the relative location of species along with the environmental variable (Palmer, 1993).

The correlation analysis was performed using the Pearson correlation coefficient and values are included in the text. The correlation chart is provided in annexure 1. In addition, the t-test was performed on *E. huxleyi* morphotypes B/C and C tube size to examine if tube size is significantly different between both morphotypes.

4. Results:

4.1 Variations in environmental parameters

A detailed variation in the environmental parameters in the study region is provided by Shetye et al. (2015). In general, a decrease in SST and SSS and an increase in nutrients (NO_3 , NO_2 , PO_4 , SiO_4) and pCO_2 concentrations are observed in the poleward direction. The nutrient concentrations and pCO_2 are higher at 48°E as compared to 57.30°E . Additionally, figs. 3 and 4 also show a decrease in CO_3^{2-} concentrations (282-107 $\mu\text{mol/kg}$) in the cooler high latitude waters.

4.2 *E. huxleyi* morphotypes composition in the Indian sector of the Southern Ocean

The analysis revealed that *E. huxleyi* abundances in the Indian sector of the Southern Ocean (transects at 57.3°E, and 48°E; between 38°S and 60°S) were dominated by *E. huxleyi* morphotype C, followed by morphotypes B/C and A. The % abundance compositions of *E. huxleyi* morphotypes at 57.3°E and 48°E transect were, morphotype A 2.1% and 0.5%, morphotype B/C 19.1% and 17.2%, and morphotype C 78.1% and 82.1% respectively. The higher abundances of *E. huxleyi* morphotype A documented as far as the SAZ (~45°S-53°S), however *E. huxleyi* morphotypes B/C and C were documented as far south as 59°S (Patil et al., 2020).

4.3 *Emiliana huxleyi* size variations

A total of >4250 coccoliths and >1700 *E. huxleyi* coccospheres were visually identified and analyzed for morphometric parameters. Overall, the average *E. huxleyi* coccolith size decreased from north to south. *Emiliana huxleyi* coccoliths average length (DL and CL) was larger in the ARFZ and the STZ and reduced in the SAZ and PFZ. However, a slight increase in DL and CL of morphotype C coccoliths was documented in the southernmost stations located in the PFZ (Figs. 3-6) (Table. 2). Average DL of *E. huxleyi* coccoliths in the study region measured between 2.62 μm and 3.27 μm . The DL of *E. huxleyi* coccoliths at 57.3°E ranged between, morphotype A, 2.76 μm and 3.28 μm ; morphotype B/C, 2.96 μm and 3.70 μm ; and morphotype C, 2.44 μm and 2.75 μm ; and at 48°E coccolith DL varied between, morphotype A, 2.83 μm and 3.16 μm ; morphotype B/C, 2.93 μm and 3.26 μm ; and morphotype C, 2.47 μm and 2.82 μm . The average CL of coccoliths ranged between 1.45 μm and 1.04 μm . The CL of *E. huxleyi* coccoliths at 57.3°E ranged between, morphotype A, 1.54 μm and 1.02 μm ; morphotype B/C, 1.50 μm and 1.16 μm ; and morphotype C, 1.16 μm and 0.97 μm ; and at 48°E coccolith CL varied between, morphotype A, 1.23 μm and 1.10 μm ; morphotype B/C, 1.31 μm and 1.12 μm ; and morphotype C, 1.07 μm and 0.96 μm (Figs. 3, 4) (Table 2).

Emiliana huxleyi coccospheres with a larger surface area documented in the SAF and are comprised of numerous coccoliths. On the contrary, coccospheres located at the ARFZ, STZ, and PFZ were smaller and consist of fewer coccoliths (e.g., Figs. 3, 4). The exception was the southernmost stations located in the PFZ, where the increase in average coccosphere surface area, DL, and numbers of coccoliths per coccosphere were documented. In this study, *E. huxleyi* coccosphere surface area measured ranged between 17.94 μm^3 and 43.12 μm^3 and the number of coccoliths per coccosphere counted were 15 to 28. *Emiliana huxleyi* morphotypes coccosphere surface area at 57.3°E varied between, morphotype A, 21.14 μm^3 and 22.84 μm^3 ; morphotype B/C, 21.22 μm^3 and 33.41 μm^3 ; and morphotype C, 17.72 μm^3 and 52.38 μm^3 , and at 48°E it varied between, morphotype A, 20.74 μm^3

and $26.63 \mu\text{m}^3$; morphotype B/C, $16.97 \mu\text{m}^3$ and $40.33 \mu\text{m}^3$; and morphotype C, $18.62 \mu\text{m}^3$ and $45.30 \mu\text{m}^3$. The *E. huxleyi* morphotype A coccospheres consist on average of 12-22 coccoliths; morphotype B/C consist of 12-24; whereas morphotype C possessed 16-36 coccoliths (Figs. 3, 4).

4.4 *Emiliana huxleyi* coccolith and coccosphere mass

Average *E. huxleyi* coccolith mass calculated at 57.3°E was 1.11 ± 0.35 pg (average + stdev) and at 48°E was 0.75 ± 0.17 pg. *Emiliana huxleyi* morphotypes A, B/C and C coccolith mass at 57.3°E varied between 1.14 pg and 1.90 pg, 1.05 pg and 2.06 pg, and 0.59 pg and 0.85 pg, respectively; whereas at 48°E coccolith mass varied between 1.22 pg and 1.70 pg, 1.02 pg and 1.46 pg, and 0.61 pg and 0.91 pg respectively (Figs. 5, 6).

The coccolith mass and the number of coccoliths per coccosphere were used to calculate the average mass of coccosphere. The average mass of coccosphere estimated was 21.41 ± 5.8 pg at 57.3°E , and 16.20 ± 3.20 pg at 48°E . *Emiliana huxleyi* morphotypes A, B/C and C coccosphere mass at 57.3°E varied between 18.26 pg and 35.49 pg, 14.42 pg and 34.35 pg, and 9.18 pg and 23.94 pg, respectively; whereas at 48°E varied between 17.67 pg and 26.08 pg, 16.90 pg and 32.68 pg, and 11.95 pg and 21.79 pg respectively (Figs. 5, 6).

4.5 *Emiliana huxleyi* coccolith overcalcification

The *E. huxleyi* morphotypes located in the SAZ and PFZ were weakly calcified; however, the *E. huxleyi* coccospheres captured from the stations located in the southern part of the PFZ (56°S - 58°S in the present study) showed an increase in coccolith and coccosphere size. The *E. huxleyi* coccospheres documented in these regions showed precipitation of calcite minerals on their tests (Plate 1). The Energy Dispersive Spectrometry (EDS) analysis showed the high amount of magnesium (Mg) (e.g. weight 4.11%) incorporation in the overcalcified *E. huxleyi* coccospheres and coccoliths which was much higher compared to the regular *E. huxleyi* coccospheres and coccoliths (e.g., weight 0.02%) (Fig. 7) documented in the STF-SAF regions.

4.6 *Emiliana huxleyi* tube thickness

Generally, *E. huxleyi* coccolith tube thickness varied between $0.50 \mu\text{m}$ and $0.21 \mu\text{m}$. The tube thickness was largest in the *E. huxleyi* morphotypes A and B/C ($0.5 \mu\text{m}$ - $0.32 \mu\text{m}$) and smaller in the morphotype C ($0.35 \mu\text{m}$ - $0.21 \mu\text{m}$). A gradual decrease in coccolith tube thickness was documented from the north towards the south (Fig. 8).

4.7 Statistical analysis

Overall, environmental parameters showed a strong correlation between CO_3^{2-} , NO_3 , PO_4 , SiO_4 , SST, SSS and moderate to weak correlation with pCO_2 and SiO_4 (Annexure table 1). Along the 57.3E transect *E. huxleyi* morphotypes A and B/C DL and CL showed a strong positive correlation with CO_3^{2-} , SST, and SSS and a strong negative correlation with NO_3 and PO_4 . The *E. huxleyi* morphotype A CL and DL also showed a moderate positive correlation with SiO_4 and a moderate negative correlation with pCO_2 . The *E. huxleyi* morphotype A coccolith mass showed a strong positive correlation with CO_3^{2-} , pCO_2 , SiO_4 , and SST, whereas morphotype B/C coccolith mass showed a moderate positive correlation with pCO_2 , SST, and SSS and negative correlation with NO_3 and PO_4 . No significant relationship between *E. huxleyi* morphotype C DL, CL, and coccolith, coccosphere mass with environmental parameters was documented. The *E. huxleyi* morphotype A tube size showed moderate correlation with SST; whereas, *E. huxleyi* morphotypes B/C and C tube size showed a strong positive correlation with CO_3^{2-} , SST, SSS and strong negative correlation with NO_3 and PO_4 .

Along the 48°E transect, *E. huxleyi* morphotype A DL and CL showed strong positive correlation with CO_3^{2-} , SiO_4 , SST, and SSS and strong negative correlation with NO_3 and PO_4 , however, morphotypes B/C and C showed very weak/no correlation with environmental parameters. The *E. huxleyi* morphotype A coccolith mass showed moderate to strong positive correlation with CO_3^{2-} , SiO_4 , SST, and SSS and moderate to high negative correlation with pCO_2 , NO_3 , and PO_4 . No/very weak correlation was documented between *E. huxleyi* morphotypes B/C and C coccolith mass and environmental parameters. The *E. huxleyi* morphotype A tube size showed a strong positive correlation with CO_3^{2-} , SiO_4 , and SST and a strong to moderate negative correlation with pCO_2 , NO_3 , and PO_4 . A moderate positive relationship was documented between *E. huxleyi* morphotypes B/C and C tube size and CO_3^{2-} and moderate negative correlation with NO_3 and PO_4 .

The CCA stations and *E. huxleyi* morphometrics biplots were provided separately for each studied transects. In both transects *E. huxleyi* morphotype A morphometrics (average no of coccoliths/sphere; coccolith and coccosphere mass; DL; CL, coccosphere size; and tube size) were influenced by the elevated SST, SSS, and CO_3^{2-} concentrations, whereas, morphometric measurements of morphotypes B/C and C were related to high nutrient, and low SST, SSS, CO_3^{2-} concentrations.

The t-test performed on *E. huxleyi* morphotypes B/C and C tube thickness showed significant variation in 57.3°E ($P=2.47\text{E}-08$) and 48°E ($P=1.91\text{E}-07$) transects.

5 Discussion

5.1 Biogeographical distribution of *E. huxleyi* morphotypes and their carbonate contribution

In the modern Indian sector of the Southern Ocean, *E. huxleyi* morphotype A occurs frequently in the warmer STZ (Mohan et al., 2008; Patil et al., 2014, 2017, 2020) and moderate-to-weakly calcified *E. huxleyi* morphotypes B/C (Antarctic type, Young et al., 2003; Cubillos et al., 2007), and C dominate in the SAZ and PFZ (Mohan et al., 2008; Patil et al., 2014, 2017, 2020). Among *E. huxleyi* morphotypes, morphotype C represents the most abundant in the Indian Sector of the Southern Ocean followed by morphotypes B/C and A (Mohan et al., 2008; Patil et al., 2020). All the three *E. huxleyi* morphotypes are characterized by different coccolith morphologies, degree of calcification (Young and Ziveri, 2000; Poulton et al., 2007), and probably belong to the different taxonomic varieties. However, *E. huxleyi* morphotypes B/C and C represent similar ecological niches, as they show similar seasonal distribution (Young et al., 2003; Mohan et al., 2008; Patil et al., 2020; Rigual-Hernández et al., 2020) but differ significantly concerning coccolith production, morphologies and mass (Patil et al., 2020; Rigual-Hernández et al., 2020) (figs. 5,6). The investigations on *E. huxleyi* morphotypes production, biogeographic expanse, calcite production, and response to changes in the Southern Ocean physico-chemical conditions are thus crucial to evaluate their response to projected environmental changes and hence impact on biogeochemical cycles (Deepeler et al., 2017).

Overall, all *E. huxleyi* morphotypes show decreasing coccolith length and mass from the SSTF to PF which indicate a response to changes in the physico-chemical conditions and oceanographic settings. Though *E. huxleyi* morphotypes A and B/C represent different ecological niches (Figs. 9a, b), a strong and significant correlation is documented between *E. huxleyi* morphotypes A and B/C morphometrics, and CO_3^{2-} , NO_3 , SST, and SSS in the 48°E and 57.3°E transects (Annexure table 1, 2). Similarly, *E. huxleyi* morphotypes A and B/C coccolith mass is correlated with CO_3^{2-} , pCO_2 , SST, and SSS, however, the extent of this correlation was significantly different in both transects (Annexure table 1, 2). Additionally, our results signify that SiO_4 and pCO_2 may act as crucial controls in *E. huxleyi* morphotype A production, morphometrics, and calcite production (Rigual-Hernández et al., 2020). On the other hand, though *E. huxleyi* morphotype C represents similar biogeographic distribution as *E. huxleyi* morphotype B/C it is not well correlated with the environmental gradients, probably due to its narrow size range compared to *E. huxleyi* morphotypes B/C and A (figs. 3-4, Table 2). We suggest that multiple environmental and oceanographic factors may affect each *E. huxleyi* morphotype differently resulting in variations in their growth, morphologies, and calcification rates (Figs. 3-6 Annexure tables 1, 2).

In earlier studies, a wide range of environmental parameters (viz. temperature, salinity, irradiance, CO₂, NO₃, PO₄, etc.) were recognized to influence *E. huxleyi* morphotypes growth, calcification rates (Zondervan et al., 2007; Feng et al., 2017). Few studies attributed variation in *E. huxleyi* coccolith size to changes in the seawater salinity (e.g., Bollmann and Herrle, 2007; Bollmann et al., 2009). This study documents smaller *E. huxleyi* coccospheres in the SSTF and PF containing larger coccoliths, and larger coccosphere in the SAF containing smaller coccoliths (Figs. 3-5). A strong correlation between *E. huxleyi* morphotypes A, B/C, and SSS along the 57.3°E transect, moderate-weak correlation with morphotype A in the 48°E transect, and no correlation with morphotype C indicates, the change in *E. huxleyi* morphotypes morphologies are not controlled by SSS alone (Annexure tables 1, 2). The SSS may act as the crucial factor for change in coccolith morphologies, however, the response may vary with morphotypes/strains (Gebühr et al., 2021). This is probably one of the reasons for the increase in coccolith and coccosphere size in the southernmost stations. The larger coccospheres of *E. huxleyi* morphotypes C and B/C in the SAZ comprising small but numerous coccoliths are probably caused by sudden increases in nutrients (NO₃, PO₄) and decreases in SSS and SST. These large-sized *E. huxleyi* morphotypes C and B/C coccospheres at the SAZ comprise higher mass than that of the *E. huxleyi* morphotype A coccospheres in the STZ (Figs. 5, 6), suggesting weakly calcified *E. huxleyi* morphotypes B/C and C can act as larger carbonate contributors to the Indian Sector of the Southern Ocean sediments compared to *E. huxleyi* morphotype A. Additionally, this study documents a good correlation of *E. huxleyi* morphotypes A and B/C with pCO₂, although it is difficult to ascertain effect of latitudinal variation in pCO₂ concentration on *E. huxleyi* morphotype production and calcification.

The comparison of two different transects (at 48°E and 57.3°E) shows that the average coccolith mass decreased from 1.11 pg at 57.3°E to 0.75 pg at 48°E. Though it seems to be a small difference, it is a decrease of 32%. Similarly, coccosphere mass decreased from 57.3°E to 48°E by 24.3%. The decrease in the coccolith (and hence coccosphere) mass is due to the reduction of CO₃²⁻ ion concentrations by 18% from 57.3°E to 48°E (e.g., Beaufort et al., 2011). Considering there is no much latitudinal difference between these two transects and since sampling was carried out in the same season, our studies indicate *E. huxleyi* species-specific carbonate contribution may vary massively in the Southern Ocean within the small geographic regions and obviously between the different Southern Ocean sectors. The change in carbonate chemistry and coccolithophore physiology (viz. production, morphology, and calcification) in both transects are linked to changes in ocean circulation and the influence of eddies. Previous studies showed that the study region is influenced by the Agulhas Retroflection Current (ARC) (Anilkumar et al., 2014; Jenson et al., 2018). The ARC influences the

SSTF and SAF along the 48°E transect, and the SSTF, SAF, and PF along the 57.3°E transect due to meandering of the Antarctic Circumpolar Current which is governed by the bottom topography (Anilkumar et al., 2014). In addition, the mid-oceanic islands probably influenced biological production along the 57.3°E transect. The frontal shifts, the influence of the ARC, and influence of the mid-oceanic islands probably responsible for differences in the macro- (e.g., NO₃, PO₄) and micronutrient concentrations (e.g., Fe, Mg), CO₃²⁻ concentration along the 57.3°E transect which thus reflected in *E. huxleyi* production as well as their morphometric variations.

5.2 *Emiliana huxleyi* coccoliths preservation and morphotypes recognition in the Southern Ocean sediments

Though *E. huxleyi* morphotypes C and B/C comprise elevated abundance (70-98% of relative abundance) in the surface waters of the Southern Ocean between the STZ and AZ, surface sediments do not favor *E. huxleyi* preservation in the SAZ and PFZ (Boeckel et al. (2006). The zooplankton grazing and mechanical breakage of coccospheres and the effect of acidic food vacuoles of zooplankton may enhance fragmentation of coccoliths and escalate calcite dissolution (e.g., Mayers et al., 2019) in the upper few hundred meters of the water column. Though the rapid sink of coccoliths in the form of marine snow increases sinking rates and readily deposition in the ocean floor (Ziveri et al., 2007) the deeper seabed/shallow Carbonate Compensation Depth dissolves coccoliths in the lower water column. The previous studies by Rigual-Hernández et al. (2020) indicate that the coccoliths in the sediment traps (located at 1000m, 2000m, and 3800m water depth) are much better preserved, whereas the poor preservation of *E. huxleyi* in the seabed is due to several processes which can alter the preservation and composition such as, supralysocline dissolution process (Milliman et al., 1999), microbial oxidation of organic matter, etc. However, the coccolith tube is robust and often documented in the surface sediments (e.g. Rigual-Hernández et al., 2020, Fig. 3a). We documented significant differences in the *E. huxleyi* morphotypes B/C and C coccolith tube size and central area in both the studied transects (i.e., t-test P=2.47E-8 along the 57.3°E transect; and P=1.91E-7 along the 48°E transect). We suggest that owing to the large range and significant difference of coccolith tube size and the central area between morphotypes B/C and C coccoliths, their morphometric studies can be applied to ocean sediments to separate the *E. huxleyi* assemblage into morphotypes B/C and C. This information will be crucial to investigate possible carbonate contribution by *E. huxleyi* B/C and C morphotypes in highly corroded/weakly preserved sediments, where visual identification of morphotypes is not feasible. Though we observed a strong correlation between *E. huxleyi* morphotypes B/C and C tube size with CO₃²⁻, SST, SSS and a strong positive correlation of *E. huxleyi* morphotype

A tube size with SST, the variation in tube size may be subjected to change in overall length of the coccolith.

5.3 Coccolithophore overcalcification at the south of the PFZ

Observational studies offer important insights about possible adaptations of coccolithophores to the increasing CO₂ and reducing ocean CO₃²⁻ concentration. A general pattern of reduction in coccolith calcite mass and coccosphere with increasing pCO₂ has been documented in the living and fossil assemblages across the world ocean basins (Beaufort et al., 2011). However, *E. huxleyi* morphotypes are often found to dominate in the regions of elevated pCO₂ (e.g. >300 µatm for the present study). For instance, *E. huxleyi* morphotype A with heavily calcified coccoliths dominate in the regions of moderate pCO₂ (e.g., 180-220 µatm for the present study) while weakly calcified morphotypes (morphotypes B/C and C) with lighter coccoliths dominate in high pCO₂ waters (i.e., 250-350 µatm for the present study) (Beaufort et al., 2011; Poulton et al., 2011). Beyond this, the dominance of over-calcified *E. huxleyi* group A morphotypes were documented in the naturally acidified upwelling waters of the Chilean upwelling zone (Beaufort et al., 2011) with pCO₂ values more than 2-fold higher than present-day levels in the atmosphere (von Dassow et al., 2018). Similarly, in the Bay of Biscay *E. huxleyi* morphotype A overcalcified coccospheres were documented during winter when pCO₂ was highest (Smith et al., 2012; Rigual-Hernández et al., 2020). The probable explanations are that the heavily calcified forms are especially tolerant to the higher pCO₂ levels (von Dassow et al., 2018). In this study, large *E. huxleyi* morphotypes B/C and C coccoliths located in the cold, low CO₃²⁻, and high pCO₂ concentrations (>350 µmol/kg) (Figs. 3-6) show extracellular calcite mineralization with a high percentage of Mg incorporation indicating secondary calcification may occur naturally in living *E. huxleyi* coccolithophores. Similar calcification was seen in *E. huxleyi* morphotype B/C coccoliths in the Australian sector of the Southern Ocean at 61°S site located in the Antarctic Zone (Rigual-Hernández et al., 2018, Plate 1e-g) which was interpreted as precipitation of salt over the organic coccolith scaffold that resulted to coccolith dissolution. We hypothesize that the overcalcification of *E. huxleyi* coccoliths in the southernmost stations are governed by external calcite mineralization controlled by polysaccharides extruded along with coccoliths, decreasing temperature, and high pCO₂ levels. *Emiliana huxleyi* living in this stressful environment (e.g. southern high latitudes) probably releases excess EPS for the cryoprotection which acts as a binder for Ca, Mg ions on coccospheres. For instance, in the presence of (positive) divalent cations (e.g., Ca²⁺, Mg²⁺) polysaccharides can form cation bridges with adjacent polymers having also negative functional groups (Decho and Gutierrez, 2017) and cause extracellular crystal nucleation. In addition, the EPS concentration is higher in the high latitude waters during the austral summer period derived from algae

and sea ice bacteria (Underwood et al., 2010) which possibly helps in enhancing excess extracellular Ca, Mg binding/precipitation. Additionally, we suspect *E. huxleyi* (irrespective of morphotype, since all *E. huxleyi* morphotypes are genetically closely related) possess the ability to cope with decreasing CO_3^{2-} levels. The weakly calcified *E. huxleyi* morphotypes C and B/C, similar to the heavily calcified *E. huxleyi* morphotypes, can also opt for external mineralization as a protective measure. However, further investigations are needed to understand if coccolithophore cells can play any role in controlling extracellular Ca and Mg mineralization on coccospheres.

Similar to the Indian sector (current study) and Australian sector of the Southern Ocean (Rigual-Hernández et al., 2018), *E. huxleyi* overcalcification may be prominent in the other sectors of the Southern Ocean and also in the upwelling regions where pCO_2 concentration is high (>350-400 μatm). We suggest that apart from the role of polysaccharides, lowering pH, pCO_2 , and other factors such as temperature probably play a role in overcalcification/extracellular mineralization. For instance, recently Nash et al. (2019) have shown high Mg content in the outer rings of coralline algae and have related it to the rise in ocean temperature. In addition, a recent model study on coccolithophores predicted that in the future climate change scenario (specifically in lowering oceanic pH), coccolithophores may adopt a slow-growth strategy and get more heavily calcified, possibly due to better carbon fixation ability (Irie et al., 2010).

In the previous study, Rigual-Hernández et al. (2018) documented a gradually decreasing trend in coccolith length and weight from mid-February to winter with the largest length appearing during August. This indicates that coccoliths are larger in colder, nutrient-rich waters with low carbonate concentration [CO_3^{2-}] and low calcite saturation levels (Ω_{calcite}), implying *E. huxleyi* may have better adaptability to changing carbonate chemistry than previously thought. Owing to the better adaptability of *E. huxleyi* in wide environmental conditions, they can be better adapted to future CO_3^{2-} , temperature, and salinity changes (Winter et al., 2014). However, other physical (i.e., seasonal reversal of winds and currents, upwelling, mixing, seasonal temperature, and salinity variation) and biological factors (e.g., productivity) may play a crucial role in regulating calcification mechanisms and these factors can influence ocean pH to a large extent, thus may need rigorous investigation. Previous studies indicated the threat of ocean acidification on marine calcifiers depositing calcium carbonate minerals possessing a significant proportion of magnesium ions (ie. magnesium calcite) (Orr et al., 2005; Roberts et al., 2006; Turley et al., 2007; Kuffner et al., 2008). We suggest that though the addition of Mg will make the coccolith more soluble but more importantly it will increase the coccolith mineral hardness. This could be a protective mechanism by the coccoliths to counter grazing. Thus it would be

interesting to see whether coccolithophores in upcoming decades prefers to decrease their solubility or to increase their coccolith hardness.

6 Conclusions

- Our *E. huxleyi* morphometric measurements indicate changes in the coccolith, coccosphere size, and mass variation in the Indian sector of the Southern Ocean from the STZ to PFZ. The *E. huxleyi* coccospheres located in the SSTF are small in size comprising fewer but larger coccoliths; whereas, the coccospheres located in the SAZ are large consisting of small but numerous coccoliths. Our study revealed that ‘Group B’ morphotypes (morphotypes B/C and C) located in the SAZ, owing to their large surface area and a large number of coccoliths per coccosphere, contribute a large amount of CaCO₃ to the Southern Ocean sediments compared to ‘Group A’ morphotypes located in the STZ. The morphology of coccoliths and carbonate contribution vary largely within and between the Southern Ocean sectors as feedback of changes in the in-situ environmental conditions.
- The morphometric studies indicate a large difference in *E. huxleyi* morphotypes B/C and C coccolith central area which can be useful to distinguish between *E. huxleyi* morphotypes B/C and C in the Southern Ocean sediments where coccoliths are highly corroded and morphotypes are not recognizable.
- *Emiliania huxleyi* coccospheres located in the cold, nutrient-rich PFZ waters are large, heavily calcified suggesting extracellular Ca mineralization with the presence of a large amount of Mg. This indicates the possibility of *E. huxleyi* getting adapted to low pH, high pCO₂ conditions through extracellular calcite mineralization, thus indicating an adaptive mechanism to cope with changing carbonate chemistry in the future.

Acknowledgments

We are grateful to the Secretary, Ministry of Earth Sciences, New Delhi, and the Director NCPOR, Goa, for their constant encouragement and support under the project “Polar Micropaleontology and Past Climate”. Dr. Shramik would like to thank DST-INSPIRE for providing funds for the project DST/INSPIRE/04/2015/001969. This is NCPOR contribution No. -----

References

- Andersson, A.J., Mackenzie, F.T., Bates, N.R., 2008. Life on the margin: implications of ocean acidification on Mg-calcite, high latitude and cold-water marine calcifiers. *Marine Ecology Progress Series*, 373, 265-273. <https://doi.org/10.3354/meps07639>.
- Anilkumar, N., George, J.V., Chacko, R., Nuncio, N., Sabu, P., 2014. Variability of fronts, fresh water input and chlorophyll in the Indian Ocean sector of the Southern Ocean. *New Zealand Journal of Marine and Freshwater Research*. <https://dx.doi.org/10.1080/00288330.2014.924972>.
- Anilkumar, N., Luis, A.J., Somayajulu, Y.K., Babu, V.R., Dash, M.K., Pednekar, S.M., Babu, K.N., Sudhakar, M., Pandey, P.C., 2006. Fronts, water masses and heat content variability in the Western Indian sector of the Southern Ocean during austral summer 2004. *Journal of Marine Systems*, 63(1-2), 20-34. <https://doi.org/10.1016/j.jmarsys.2006.04.009>.
- Balch, W.M., Bates, N.R., Lam, P.J., Twining, b.S., Rosengard, S.Z., Bowler, B.C., Drapeau, D.T., Garley, R., Lubelczyk, L.C., Mitchell, C., Rauschenberg, S., 2016. Factors regulating the great calcite Belt in the Southern Ocean and its biogeochemical significance, *Global Biogeochem Cycles* 30(8), 1124-1144. <https://doi.org/10.1002/2016GB005414>.
- Balch, W.M., Drapeau, D.T., Bowler, B.C., Lyczkowski, E., Booth, E.S., Alley, D., 2011. The contribution of coccolithophores to the optical and inorganic carbon budgets during the Southern Ocean Gas Exchange Experiment: New evidence in support of the “Great Calcite Belt” hypothesis, *Journal of geophysical Research-Oceans*, 116, C00F06. <https://doi.org/10.1029/2011JC006941>.
- Beaufort, L., Probert, I., de Garidel-Thoron, T., Bendif, E.M., Ruiz-Pino, D., Metzl, N., Goyet, C., Buchet, N., Coupel, P., Grelaud, M., Rost, B., Rickaby, R.E.M., de Vargas, C., 2011. Sensitivity of coccolithophores to carbonate chemistry and ocean acidification, 476, 80-83. <https://doi.org/10.1038/nature10295>.
- Bijma, J., Hönisch, B., Zeebe, R.E., 2002. Impact of the ocean carbonate chemistry on living foraminiferal shell weight: Comment on “Carbonate ion concentration in glacial-age deep waters of the Caribbean Sea” by W.S., Broecker and E. Clark. *Geochemistry, Geophysics, Geosystems*, 3, 1-7. <https://doi.org/10.1029/2002GC003888>.
- Boeckel, B., Baumann, K.-H., 2008. Vertical and lateral variations in coccolithophore community structure across the subtropical frontal zone in the South Atlantic Ocean. *Marine Micropaleontology*, 67, 255-273. <https://doi.org/10.1016/j.marmicro.2008.01.014>.
- Boeckel, B., Baumann, K.-H., Henrich, R., Kinkel, H., 2006. Coccolith distribution patterns in South Atlantic and Southern Ocean surface sediments in relation to environmental gradients. *Deep Sea Research I*, 53, 1073-1099. <https://doi.org/10.1016/j.dsr.2005.11.006>. Bollmann, J., Herrle, J.O., 2007. Morphological variation of *Emiliania huxleyi* and sea surface salinity. *Earth and Planetary Science Letters*, 255, 273-288. <https://doi.org/10.1016/j.epsl.2006.12.029>.
- Bollmann, J., Herrle, J.O., Cortés, M.Y., Fielding, S.R., 2009. The effect of sea water salinity on the morphology of *Emiliania huxleyi* in plankton and sediment samples. *Earth and Planetary Science Letters*, 284, 320-328. <https://doi.org/10.1016/j.epsl.2009.05.003>.
- Brown, C.W., Yoder, J.A., 1994. Coccolithophorid blooms in the global ocean. *Journal of Geophysical Research: Oceans*, 99, 7467-7482. <https://doi.org/10.1029/93JC02156>.

- Caldeira, K., Wickett, M., 2003. Anthropogenic carbon and ocean pH. *Nature* 425, 365. <https://doi.org/10.1038/425365a>.
- Cao, L., Caldeira, K., 2008. Atmospheric CO₂ stabilization and ocean acidification. *Geophysical Research Letters*, 35(19), L19609. <https://doi.org/10.1029/2008GL035072>.
- Charalampopoulou, A., Poulton, A.J., Bakker, D.C.E., Lucas, M. I., Stinchcombe, M.C., Tyrrell, T., 2016. Environmental drivers of coccolithophore abundance and calcification across Drake Passage (Southern Ocean). *Biogeosciences*, 13, 5917– 5935. <https://doi.org/10.5194/bg-13-5917-2016>
- Cook, S.S., Jones, R.C., Vaillancourt, R.E., Hallegraeff, G.M., 2013. Genetic differentiation among Australian and Southern Ocean populations of the ubiquitous coccolithophore *Emiliana huxleyi* (Haptophyta), *Phycologia*, 52, 368-374. <https://doi.org/10.2216/12-111.1>.
- Cook, S.S., Whittock, L., Wright, S.W., Hallegraeff, G.M., 2011. Photosynthetic pigment and genetic difference between two southern ocean morphotypes of *Emiliana huxleyi* (haptophyta), *Journal of Phycology*, 47, 615-626. <https://doi.org/10.1111/j.1529-8817.2011.00992.x>.
- Cubillos, J., Wright, S., Nash, G., De Salas, M., Griffiths, B., Tilbrook, B., Poisson, A., Hallegraeff, G., 2007. Calcification morphotypes of the coccolithoporid *Emiliana huxleyi* in the Southern Ocean: changes in 2001 to 2006 compared to historical data, *Marine Ecology Progress Series*, 348, 47-54. <https://doi.org/10.3354/meps07058>.
- Decho, A.W., Gutierrez, T., 2017. Microbial Extracellular Polymeric Substances (EPSs) in Ocean Systems. 8, 922. <https://doi.org/10.3389/fmicb.2017.00922>.
- Deepeler, S.L., Davidson, A.T., 2017. Southern Ocean Phytoplankton in a Changing Climate. *Frontiers in Marine Science*, 4:40. <https://doi.org/10.3389/fmars.2017.00040>.
- Engel, A., Zondervan, I., Aerts, K., Beaufort, L., Benthien, A., Chou, L., Delille, B., Gattuso, J.-P., Harlay, J., Heemann, C., Hoffmann, L., Jacquet, S., Nejstgaard, J., Pizay, M.-D., Rochelle-Newall, E., Schneider, U., Terbrueggen, A., Riebesell, U., 2005. Testing the direct effect of CO₂ concentration on a bloom of the coccolithophorid *Emiliana huxleyi* in mesocosm experiments, *Limnology and Oceanography*, 50(2), 493-507. <https://doi.org/10.4319/lo.2005.50.2.0493>.
- Fabry, V.J., McClintock, J.B., Mathis, J.T., Grebmeier, J.M., 2009. Ocean Acidification at High Latitudes: The Bellweather. *Oceanography*, 22, 160-171. <https://doi.org/10.5670/oceanog.2009.105>.
- Feely, R.A., Doney, S.C., Cooley, S.R., 2009. Ocean acidification: present conditions and future changes in a High-CO₂ world. *Oceanography*, 22, 36-47. <https://doi.org/10.5670/oceanog.2009.95>.
- Feely, R.A., Sabine, C.L., Lee, K., Berelson, W., Kleypas, J., Fabry, V.J., Millero, F.J., 2004. Impact of Anthropogenic CO₂ on the CaCO₃ System in the Oceans. *Science*, 305(5682), 362-366. <https://doi.org/10.1126/science.1097329>.

- Feng, Y., Roleda, M.Y., Armstrong, E., Boyd, P.W., Hurd, C.L., 2017. Environmental controls on the growth, photosynthetic and calcification rates of a Southern Hemisphere strain of the coccolithophore *Emiliana huxleyi*. *Limnology and Oceanography*, 62, 519-540. <https://doi.org/10.1002/Lno. 10442>.
- Feng, Y., Warner, M.E., Zhang, Y., Sun, J., Fu, F.X., Rose, J.M., Hutchins, D.A., 2008. Interactive effects of increased pCO₂, temperature and irradiance on the marine coccolithophore *Emiliana huxleyi* (Prymnesiophyceae). *European Journal of Phycology*, 43, 87-98. <https://dx.doi.org/10.1080/09670260701664674>.
- Findlay, C.S., Giraudeau, J., 2000. Extant calcareous nannoplankton in the Australian Sector of the Southern Ocean (austral summer 1994 and 1995). *Marine Micropaleontology*, 40(4), 417-439. [https://doi.org/10.1016/S0377-8398\(00\)00046-3](https://doi.org/10.1016/S0377-8398(00)00046-3).
- Fiorini, S., Middelburg, J.J., Gattuso, J.-P., 2011. Testing the effects of elevated PCO₂ on coccolithophores (Prymnesiophyceae): comparison between Haploid and Diploid life stages(1), *Journal of Phycology*, 47(6), 1281-1291. <https://doi.org/10.1111/j.1529-8817.2011.01080.x>.
- Freeman, N.M., Lovenduski, N.S., 2015. Decreased calcification in the Southern Ocean over the satellite record. *Geophysical Research Letters*, 42, 1834-1840. <https://dx.doi.org/10.1002/2014GL062769>.
- Gandhi, N., Ramesh, R., Laskar, A.H., Sheshshayee, M.S., Shetye, S., Anilkumar, N., Patil, S.M., Mohan, R., 2012. Zonal variability in primary production and nitrogen uptake rates in the southwestern Indian Ocean and the Southern Ocean, *Deep Sea Research I*, 67, 32-43. <https://doi.org/10.1016/j.dsr.2012.05.003>.
- Gebühr, C., Sheward, R.M., Herrle, J.O., Bollmann, J., 2021. Strain-specific morphological response of the dominant calcifying phytoplankton species *Emiliana huxleyi* to salinity change. *PLoS ONE*, 16(2), e0246745. <https://doi.org/10.1371/journal.pone.0246745>.
- George, J.V., Anilkumar, N., Nuncio, M., Soares, M.A., Naik, R.K., Tripathy, S.C., 2018. Upper layer diapycnal mixing and nutrient flux in the subtropical frontal region of the Indian sector of the Southern Ocean. *Journal of Marine Systems*, 187, 197-205. <https://doi.org/10.1016/j.jmarsys.2018.07.007>.
- Grasshoff, K., Ehrhardt, M., Kremling, K., 1983. *Methods of Seawater Analysis*. Verlag Chemie, Weinheim, p. 419.
- Hagino, K., Bendif, E.M., Young, J.R., Kogame, K., Probert, I., Takano, Y., Horiguchi, T., de Vargas, C., Okada, H., 2011. New evidence for morphological and genetic variation in the cosmopolitan coccolithophore *Emiliana huxleyi* (Prymnesiophyceae) from the COX1b-ATP4 genes, *Journal of Phycology*, 47(5), 1164-1176. <https://doi.org/10.1111/j.1529-8817.2011.01053.x>.
- Holligan, P.M., Charalampopoulou, A., and Hutson, R., 2010. Seasonal distributions of the coccolithophore, *Emiliana huxleyi*, and of particulate inorganic carbon in surface waters of the Scotia Sea. *Journal of Marine Systems*, 82(4), 195-205. <https://doi.org/10.1016/j.jmarsys.2010.05.007>.

- Iglesias-Rodríguez, M.D., Halloran, P.r., Rickaby, R.E.M., Hall, I.R., Colamenero-Hidalgo, E., Gittins, j.R., Green, D.R.H., Tyrrell, T., Gibbs, S.J., von Dassow, P., Rehm, E., Armbrust, E.V., Boessenkool, K.P., 2008. Phytoplankton calcification in a high-CO₂ world, *Science*, 320, 336-340. <https://doi.org/10.1126/science.1154122>.
- IPCC. 2019. Summary for policymakers. In: Pörtner, H.O., Roberts, D.C., Masson-Delmotte, V., Zhai, P., Tignor, M., Poloczanska, E., Mintenbeck, K., Alegría, A., Nicolai, M., Okem, A., Petzold, J., Rama, B., Weyer, N.M. (eds.), IPCC Special report on the ocean and cryosphere in a changing climate. In press.
- IPCC. Climate Change, 2013. The Physical Science Basis. Contribution of Working Group I to the Fifth Assessment Report of the Intergovernmental Panel on Climate Change. Cambridge, United Kingdom and New York, USA, Cambridge University Press.
- Irie, T., Bessho, K., Findlay, H.S., Findlay, H.S., Calosi, P., 2010. Increasing costs due to ocean acidification drives phytoplankton to be more heavily calcified: Optimal growth strategy of coccolithophores. *PLoS ONE*, 5(10): e13436. <https://doi.org/10.1371/journal.pone.0013436>.
- Kovach, W., 2007. MVSP-A MultiVariate Statistical Package for Windows, ver 3.1. Kovach Computing Services, Pentraeth, Wales, U.K.
- Linge Johnsen, S.A., Bollmann, J., 2020. Coccolith mass and morphology of different *Emiliana huxleyi* morphotypes: A critical examination using Canary Islands material. *PLoS ONE*, 15(3), e02305669. <https://doi.org/10.1371/journal.pone.0230569>. Jones, B.M., Iglesias-Rodriguez, M.D., Skipp, P.J., Edwards, R.J., Greaves, M.J., Young, J.R., Elderfield, H., O'Connor, C.D., 2013. Response of the *Emiliana huxleyi* Proteome to Ocean Acidification, 8(4), e61868. <https://doi.org/10.1371/journal.pone.0061868>.
- Jordan, R.W., Chamberlain, A.H.L., 1997. Biodiversity among haptophyte algae. *Biodiversity and Conservation*, 6(1), 131-152. <https://doi.org/10.1023/A:1018383817777>.
- Klaas, C., Archer, D.E., 2002. Association of sinking organic matter with various types of mineral ballast in the deep sea: Implications for the rain ratio. *Global Biogeochemical Cycles*, 16(4), 63-1-63-14. <https://doi.org/10.1029/2001GB001765>.
- Kleypas, J.A., Buddemeier, R.W., Archer, D., Gattuso, J.-P., Langdon, C., Opdyke, B.N., 1999. Geochemical Consequences of Increased Atmospheric Carbon Dioxide on Coral Reefs. *Science*, 284, 118-120. <https://doi.org/10.1126/science.284.5411.118>.
- Kuffner, I.B., Andersson, A.J., Jokiel, P., Rodgers, K.S., Mackenzie, F.T., 2007. Decreases in recruitment of crustose coralline algae due to ocean acidification, *Nature Geoscience*, 1, 114-117. <https://doi.org/10.1038/ngeo100>.
- Langer, G., Nehrke, G., Probert, I., Ziveri, P., 2009. Strain-specific response of *Emiliana huxleyi* to changing seawater carbonate chemistry, *Biogeosciences*, 6, 2637-2646. <https://doi.org/10.5194/bg-6-2637-2009>.
- Lohbeck, K., Riebesell, U., Reusch, T., 2012. Adaptive evolution of a key phytoplankton species to ocean acidification. *Nature Geoscience*, 5, 346-351. <https://doi.org/10.1038/ngeo1441>.

- Malinverno, E., Triantaphyllou, M.V., Dimiza, M.D., 2015. Coccolithophore assemblage distribution along a temperate to polar gradient in the West Pacific sector of the Southern Ocean (January 2005). *Micropaleontology*, 61(6), 489-506. <https://doi.org/10.2307/44511372>.
- Manno, C., Bednaršek, N., Tarling, G.A., Peck, V.L., Comeau, S., Adhikari, D., Bakker, D.C.E., Bauerfeind, E., Bergan, A.J., Berning, M.I., Buitenhuis, E., Burrige, A.K., Chierici, M., Flöter, S., Fransson, A., Gardner, J., Howes, E.L., Keul, N., Kimoto, K., Kohnert, P., Lawson, G.I., Lischka, S., Maas, A., Mekkes, I., Oakes, R.I., Pebody, C., Peijnenburg, K.T.C.A., Seifert, M., Skinner, J., Thibodeau, P.S., Wall-Palmer, D., Ziveri, P., 2017. Shelled pteropods in peril: Assessing vulnerability in a high CO₂ ocean. *Earth-Science Reviews*, 169, 132-145. <https://doi.org/10.1016/j.earscirev.2017.04.005>.
- Matson, P.G., Ladd, T.M., Halewood, E.R., Sangodkar, R.P., Chmelka, B.F., Iglesias-Rodriguez, M.D., 2016. Interspecific differences in biogeochemical responses to thermal change in the coccolithophore *Emiliana huxleyi*. *PLoS ONE*, 11, 1-22. <https://dx.doi.org/10.1371/journal.pone.0162313>.
- Mayers, K.M.J., Poulton, A.J., Daniels, C.J., Wells, S.R., Woodward, E.M.S., Tarran, G.A., Widdicombe, C.E., Mayor, D.J., Atkinson, A., Giering, S.I.C., 2019. Growth and mortality of coccolithophores during spring in a temperate Shelf Sea (Celtic sea, April 2015). *Progress in Oceanography*, 177, 101928. <https://doi.org/10.1016/j.pocean.2018.02.024>.
- McIntyre A., Bé, A.W.H., 1967. Modern coccolithophoridae of the Atlantic Ocean – I. Placoliths and cyrtoliths. *Deep Sea Research and Oceanographic Abstracts*, 14(5), 561-597. [https://doi.org/10.1016/0011-7471\(67\)90065-4](https://doi.org/10.1016/0011-7471(67)90065-4).
- McNeil, B.I., Matear, R.J., 2008. Southern Ocean acidification: A tripping point at 450-ppm atmospheric CO₂, *PNAS*, 105(48), 18860-18864. <https://doi.org/10.1073/pnas.0806318105>.
- Medlin, L.K., Barker, G.L.A., Campbell, L., Green, J.C., Hayes, P.K., Marie, D., Wrieden, S., Vaultot, D., 1996. Genetic characterization of *Emiliana huxleyi* (Haptophyta), *Journal of Marine Systems*, 9(1-2), 13-31. [https://doi.org/10.1016/0924-7963\(96\)00013-9](https://doi.org/10.1016/0924-7963(96)00013-9).
- Milliman, J.D., Troy, P.J., Balch, W.M., Adams, A.K., Li, Y.H., Mackenzie, F.T., 1999. Biologically mediated dissolution of calcium carbonate above the chemical lysocline? *Deep Sea Research Part I: Oceanographic Research Papers*, 46, 1653-1669. [https://doi.org/10.1016/S0967-0637\(99\)00034-5](https://doi.org/10.1016/S0967-0637(99)00034-5).
- Mohan, R., Mergulhao, L.P., Guptha, M.V.S., Rajakumar, A., Thamban, M., Anilkumar, N., Sudhakar, M., Ravindra, R., 2008. Ecology of coccolithophores in the Indian sector of the Southern Ocean. *Marine Micropaleontology*, 67(1-2), 30-45. <https://doi.org/10.1016/j.marmicro.2007.08.005>.
- Müller, M.N., Trull, T.W., Hallegraef, G.M., 2015. Differing response of three Southern Ocean *Emiliana huxleyi* ecotypes to changing seawater carbonate chemistry. *Marine Ecology Progress Series*, 531, 81-90. <https://doi.org/10.3354/meps11309>.

- Orr, J.C., Fabry, V.J., Aumont, O., Bopp, L., Doney, S.C., Feely, R.A., Gnanadesikan, A., Grueter, N., Ishida, A., Joos, F., Key, R.M., Lindsay, K., Maier-Reimer, E., Matear, R., Monfray, P., Mouchet, A., Najjar, R.G., Plattner, G.-K., Rodgers, K.B., Sabine, C.L., Sarmiento, J.L., Schlitzer, R., Slater, R.D., Totterdell, I.J., Weirig, M.-F., Yamanaka, Y., Yool, A. 2005. Anthropogenic ocean acidification over the twenty-first century and its impact on calcifying organisms. *Nature*, 437, 681-686. <https://doi.org/10.1038/nature04095>.
- Orsi, A.H., Whitworth III, T., Nowlin Jr., W.D., 1995. On the meridional extent and fronts of the Antarctic Circumpolar Current, *Deep-Sea Research I*, 42(5), 641-673. [https://doi.org/10.1016/0967\(95\)00021-W](https://doi.org/10.1016/0967(95)00021-W).
- Paasche, E., 2002. A review of the coccolithophorid *Emiliana huxleyi* (Prymnesiophyceae), with particular reference to growth, coccolith formation, and calcification-photosynthesis interactions. *Phycologia*, 40(6), 503-529. <https://doi.org/10.2216/i0031-8884-40-6-503.1>.
- Palmer, M.W., 1993. Putting things in even better order: the advantages of canonical correspondence analysis. *Ecology*, 74(8), 2215-2230.
- Patil, S.M., Mohan, R., Shetye, S.S., Gazi, S., 2013. Phytoplankton abundance and community structure in the Antarctic polar frontal region during austral summer of 2009. *Chinese Journal of Oceanology and Limnology*, 31(1), 21-30. <https://doi.org/10.1007/s00343-013-1309-x>.
- Patil S.M., Mohan, R., Shetye, S.S., Gazi, S., 2014. Morphological variability of *Emiliana huxleyi* in the Indian sector of the Southern Ocean during the austral summer of 2010. *Marine Micropaleontology*, 107, 44-58. <https://doi.org/10.1016/j.marmicro.2014.01.005>.
- Patil, S.M., Mohan, R., Shetye, S.S., Gazi, S., Baumann, K.-H., Jafar, S., 2017. Biogeographic distribution of extant Coccolithophores in the Indian sector of the Southern Ocean, *Marine Micropaleontology*, 137, 16-30. <https://doi.org/10.1016/j.marmicro.2017.08.002>.
- Patil, S.M., Mohan, R., Shetye, S.S., Gazi, S., Choudhari, P., Jafar, S., 2020. Interannual changes of austral summer coccolithophore assemblages and southward expanse in the Southern Indian Ocean, *Deep Sea Research II*, <https://doi.org/10.1016/j.dsr2.2020.104765>.
- Patr3, S.M., Ritter, M.D.N., Alejandra, M., Pivel, G., Coimbra, J.C., 2018. Surviving in the water column: defining the taphonomically active zone in pelagic systems. *Palaios*, 33, 85-93. <https://dx.doi.org/10.2110/paleo.2017.032>.
- Perrin, L., Probert, I., Langer, G., Aloisi, G., 2016. Growth of the coccolithophore *Emiliana huxleyi* in light- and nutrient-limited batch reactors: relevance for the BIOSOPE deep ecological niche of coccolithophores, *Biogeosciences*, 13, 5983-6001. <https://dx.doi.org/10.5194/bg-13-5983-2016>.
- Poulton, A.J., Adey, T.R., Balch, W.M., Holligan, P.M., 2007. Relating coccolithophore calcification rates to phytoplankton community dynamics: regional differences and implications for carbon export. *Deep Sea Research II*, 54, 538-557. <https://doi.org/10.1016/j.dsr2.2006.12.003>.
- Poulton, A. J., Charalampopoulou, A., Young, J. R., Tarran, G. A., Lucas, M. I., Quartly, G. D., 2010. Coccolithophore dynamics in non-bloom conditions during late summer in the central Iceland Basin (July–August 2007). *Limnology and Oceanography*, 55, 1601–1613. <https://doi.org/10.4319/lo.2010.55.4.1601>.

- Poulton, A.J., Young, J.R., Bates, N.R., Balch, W.M., 2011. Biometry of detached *Emiliania huxleyi* coccoliths along the Patagonian Shelf. *Marine Ecology Progress Series*, 443, 1-17. <https://doi.org/10.3354/meps09445>.
- Read, J.F., Pollard, R.T., Morrison, A.I., Symon, C., 1995. On the southerly extent of the Antarctic Circumpolar Current in the south-east Pacific. *Deep Sea Research II*, 42, 933-954. [https://doi.org/10.1016/0967-0645\(95\)00061-T](https://doi.org/10.1016/0967-0645(95)00061-T).
- Richier, S., Fiorini, S., Kerros, M.E., von Dassow, P., Gattuso, J.P., 2011. Response of the calcifying coccolithophore *Emiliania huxleyi* to low pH/high pCO₂: from physiology to molecular level, *Marine Biology*, 158(3), 551-560. <https://doi.org/10.1007/s00227-010-1580-8>.
- Riebesell, U., Bach, L.T., Bellerby, R.G.J., Monsalve, J.R.B., Boxhammer, T., Czerny, J., Larsen, A., Ludwig, A., Schulz, K.G., 2017. Competitive fitness of predominant pelagic calcifier impaired by ocean acidification. *Nature Geoscience*, 10, 19-23. <https://dx.doi.org/10.1038/ngeo2854>.
- Riebesell, U., Zondervan, I., Rost, B., Tortell, P.D., Zeebe, R.E., Morel, F.M.M., 2000. Reduced calcification of marine plankton in response to increased atmospheric CO₂, 407, 364-367. <https://doi.org/10.1038/35030078>.
- Rigual-Hernández, A.S., Flores, J.A., Sierro, F.J., Fuertes, M.A., Cros, L., Trull, T.W., 2018. Coccolithophore populations and their contribution to organic carbon export during an annual cycle in the Australian sector of the Antarctic zone. *Biogeosciences*, 15(6), 1843-1862. <https://doi.org/10.5194/bg-15-1843-2018>.
- Rigual-Hernández, A.S., Sánchez-Santos, J.M., Eriksen, R., Moy, A.D., Sierro, F.J., Flores, J.A., Abrantes, F., Bostock, H., Nodder, S.D., González-Lanchas, A., Trull, T.W., 2020. Limited variability in the phytoplankton *Emiliania huxleyi* since the pre-industrial era in the Subantarctic Southern Ocean. *Anthropocene*, 31, 100254. <https://dx.doi.org/10.1016/j.ancene.2020.100254>.
- Roberts, J.M., Wheeler, A.J., Freiwald, A., 2006. Reefs of the deep: the biology and geology of cold-water coral ecosystems. *Science*, 312, 543-547. <https://doi.org/10.1126/science.1119861>.
- Saavedra-Pellitero, M., Baumann, K.-H., Flores, J.-A., Gersonde, R., 2014. Biogeographic distribution of living coccolithophores in the Pacific sector of the Southern Ocean. *Marine Micropaleontology*, 109, 1-20. <https://doi.org/10.1016/j.marmicro.2014.03.003>.
- Saavedra-Pellitero, M., Baumann, K.-H., Fuertes, M.Á., Schulz, H., Marcon, Y., Vollmar, N.M., Flores, J.-A., Lamy, F., 2019. Calcification and latitudinal distribution of extant coccolithophores across the Drake Passage during late austral summer 2016. *Biogeosciences*, 16, 3679-3702. <https://doi.org/10.5194/bg-16-3679-2019>.
- Shadwick, E.H., Tilbrook, B., Cassar, N., Trull, T.W., Rintoul, S.R., 2015. Summertime physical and biological controls on O₂ and CO₂ in the Australian Sector of the Southern Ocean. *Journal of Marine Systems*, 147, 21-28. <https://doi.org/10.1016/j.jmarsys.2013.12.008>.
- Shetye, S.S., Mohan, R., Patil, S.M., Jena, B., Chacko, R., George, J.V., Noronha, S., Singh, N., Priya, L., Sudhakar, M., 2015. Oceanic pCO₂ in the Indian sector of the Southern Ocean during the austral summer-winter transition phase. *Deep Sea Research II*, 118, 250-260. <https://dx.doi.org/10.1016/j.dsr2.2015.05.017>.

- Smith, H.E.K., Tyrrell, T., Charalampopoulou, A., Dumousseaud, C., Legge, O.J., Birchenough, S., Pettit, L.R., Garley, R., Hartman, S.E., Hartman, M.C., Sagoo, N., Daniels, C.J., Achterberg, E.P., Hydes, D.J., 2012. Predominance of heavily calcified coccolithophores at low CaCO₃ saturation during winter in the Bay of Biscay, PNAS, 109(23), 8845-8849. <https://doi.org/10.1073/pnas.1117508109>.
- Triantaphyllou, M.V., K.-H., Karatsolis, B.-T., Dimiza, M.D., Psarra, S., Skampa, E., Patoucheas, P., Vollmar, N.M., Koukousioura, O., Katsigera, A., 2018. Coccolithophore community response along a natural CO₂ gradient off Methana (SW Saronikos Gulf, Greece, NE Mediterranean). PLoS one 13, e02200012. <https://doi.org/10.1371/journal.pone.0200012>.
- Turley, C.M., Roberts, J.M., Guinotte, J.M., 2007. Corals in deep-water: Will the unseen hand of ocean acidification destroy cold-water ecosystems? Coral Reefs, 26, 445-448. <https://doi.org/10.1007/s00338-007-0247-5>.
- Tyrell, T., Young, J.R., 2009. Coccolithophores. In: Steele, J.H., Turekian, K.K., Thorpe, S.A. (Eds), Encyclopedia of Ocean Sciences. Academia Press, San Diego, pp. 3568-3576.
- Underwood, G.J.C., Fietz, S., Papadimitriou, S., Thomas, D.N., Dieckmann, G.S., 2010. Distribution and composition of dissolved extracellular polymeric substances (EPS) in Antarctic sea ice. Marine Ecology Progress Series, 404, 1-19. <https://doi.org/10.3354/meps08557>.
- Van Dassow, P., Díaz-Rosas, F., Bendif, E.M., Jaitán-Espitia, J.-D., Mella-Flores, D., Rokitta, S., John, U., Torres, R., 2018. Over-calcified forms of the coccolithophore *Emiliana huxleyi* in high-CO₂ waters are not preadapted to ocean acidification. Biogeosciences, 15, 1515-1534. <https://doi.org/10.5194/bg-15-1515-2018>.
- Winter, A., Elbrächter, M., Krause, G., 1999. Subtropical coccolithophores in the Weddell Sea. Deep-Sea Research I, 46(3), 439-449. [https://doi.org/10.1016/S0967-0637\(98\)00076-4](https://doi.org/10.1016/S0967-0637(98)00076-4).
- Winter, A., Henderiks, J., Beaufort, L., Rickaby, R.E.M., Brown, C.W., 2014. Poleward expansion of the coccolithophore *Emiliana huxleyi*. Journal of Plankton Research, 36(2), 316-325. <https://doi.org/10.1093/plankt/fbt110>.
- Young, J., Geisen, M., Cros, L., Kleijne, A., Sprengel, C., Probert, I., Østergaard, J., 2003. A guide to extant coccolithophore taxonomy. Journal of Nannoplankton Research, Special Issue I, 1-132.
- Young, J.R., Westbroek, P., 1991. Genotypic variation in the coccolithophorid species *Emiliana huxleyi*. Marine Micropaleontology, 18, 5-23. [https://doi.org/10.1016/0377-8398\(91\)90004-P](https://doi.org/10.1016/0377-8398(91)90004-P).
- Young, J.R., Ziveri, P., 2000. Calculation of coccolith volume and its use in calibration of carbonate flux estimates. Deep Sea Research II, 47(9-11), 1679-1700. [https://doi.org/10.1016/S0967-0645\(00\)00003-5](https://doi.org/10.1016/S0967-0645(00)00003-5).
- Ziveri, P., de Bernardi, B., Baumann, K.-H., Stoll, H.M., Mortyn, P.G., 2007. Sinking of coccolith carbonate and potential contribution to organic carbon ballasting in the deep ocean. Deep Sea Research Part II: Topical Studies in Oceanography, 54, 659-675. <https://doi.org/10.1016/j.dsr2.2007.01.006>.
- Zondervan, I., 2007. The effects of light, macronutrients, trace metals and CO₂ on the production of calcium carbonate and organic carbon in coccolithophores- A review. Deep Sea Research II, 54, 521-537. <https://doi.org/doi.org/10.1016/j.dsr2.2016.12.004>.

Zondervan, I., Rost, B., Riebesell, U., 2002. Effect of CO₂ concentration on the PIC/POC ratio in the coccolithophore *Emiliana huxleyi* grown under light-limiting conditions and different daylengths, *Journal of Experimental Marine Biology and Ecology*, 272(1), 55-70. [https://doi.org/10.1016/S0022-0981\(02\)00037-0](https://doi.org/10.1016/S0022-0981(02)00037-0).

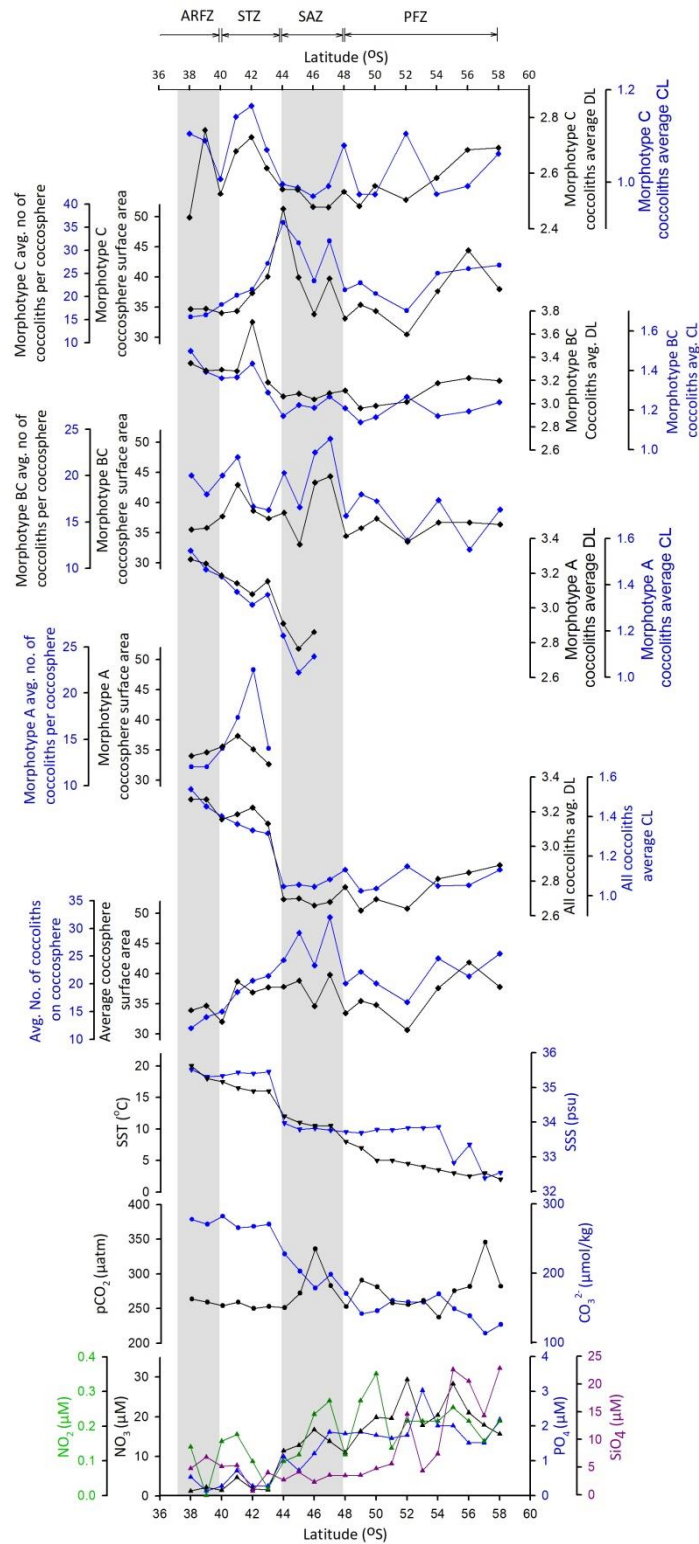


Fig. 3. Latitudinal variation in environmental parameters, *E. huxleyi* morphotypes coccolith distal shield and central area length, and average coccosphere surface area and number of coccoliths per coccosphere at 57.3°E transect. [Annotations: CL= central area length; DL= distal shield length; SST= sea surface temperature; SSS=sea surface salinity; NO₃⁻= nitrate; NO₂⁻= nitrite; PO₄³⁻= phosphate; SiO₄²⁻= silicate; PCO₂= Partial pressure of CO₂; CO₃²⁻= Carbonate concentration].

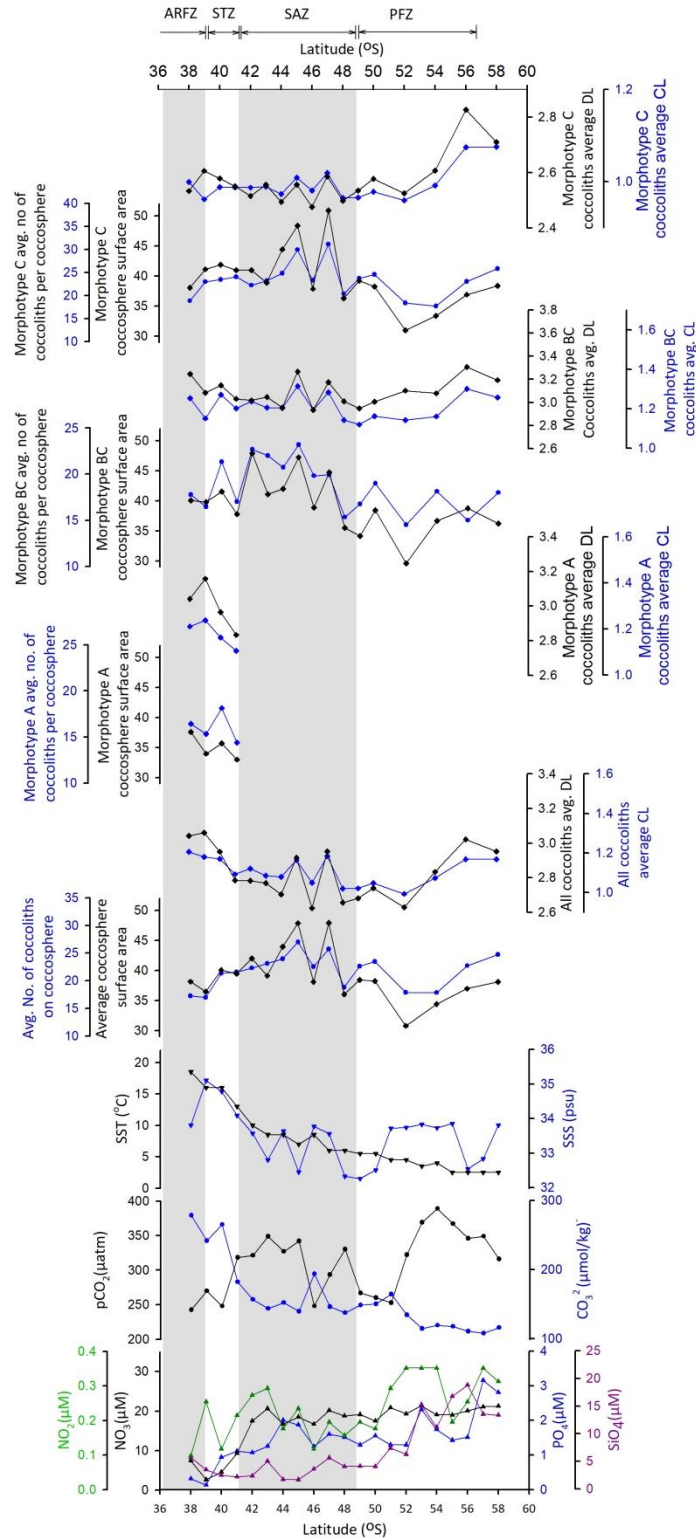


Fig. 4. Latitudinal variation in environmental parameters, *E. huxleyi* morphotypes coccolith distal shield and central area length, and average coccosphere surface area and number of coccoliths per coccosphere at 48°E transect. [Annotations: CL= central area length; DL= distal shield length; SST= sea surface temperature; SSS=sea surface salinity; NO₃= nitrate; NO₂= nitrite; PO₄= phosphate; SiO₄= silicate; PCO₂= Partial pressure of CO₂; CO₃²⁻= Carbonate concentration].

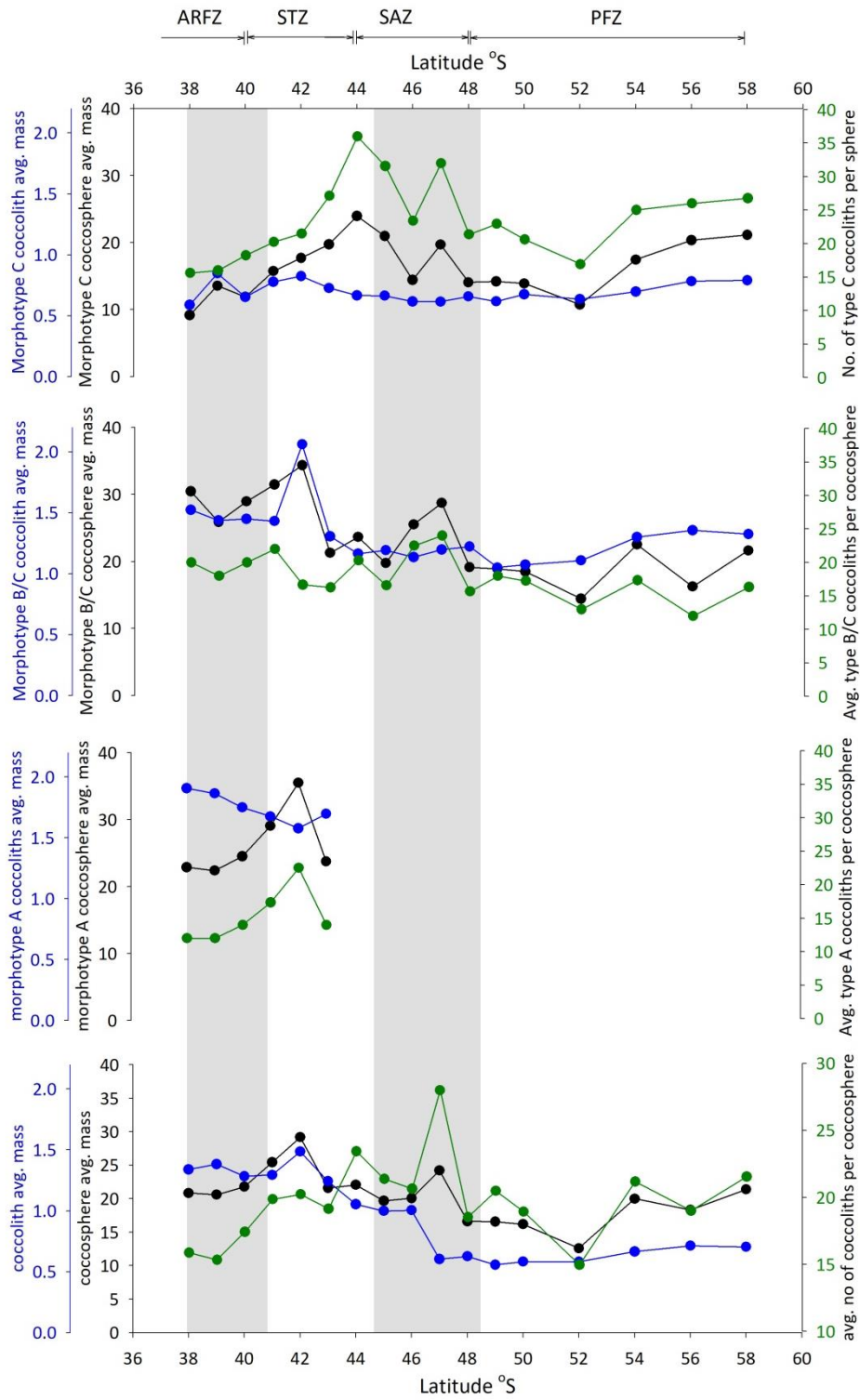


Fig. 5. *Emiliana huxleyi* coccolith and coccosphere mass (in picogram), and number of coccoliths per coccosphere documented at 57.3°E transect.

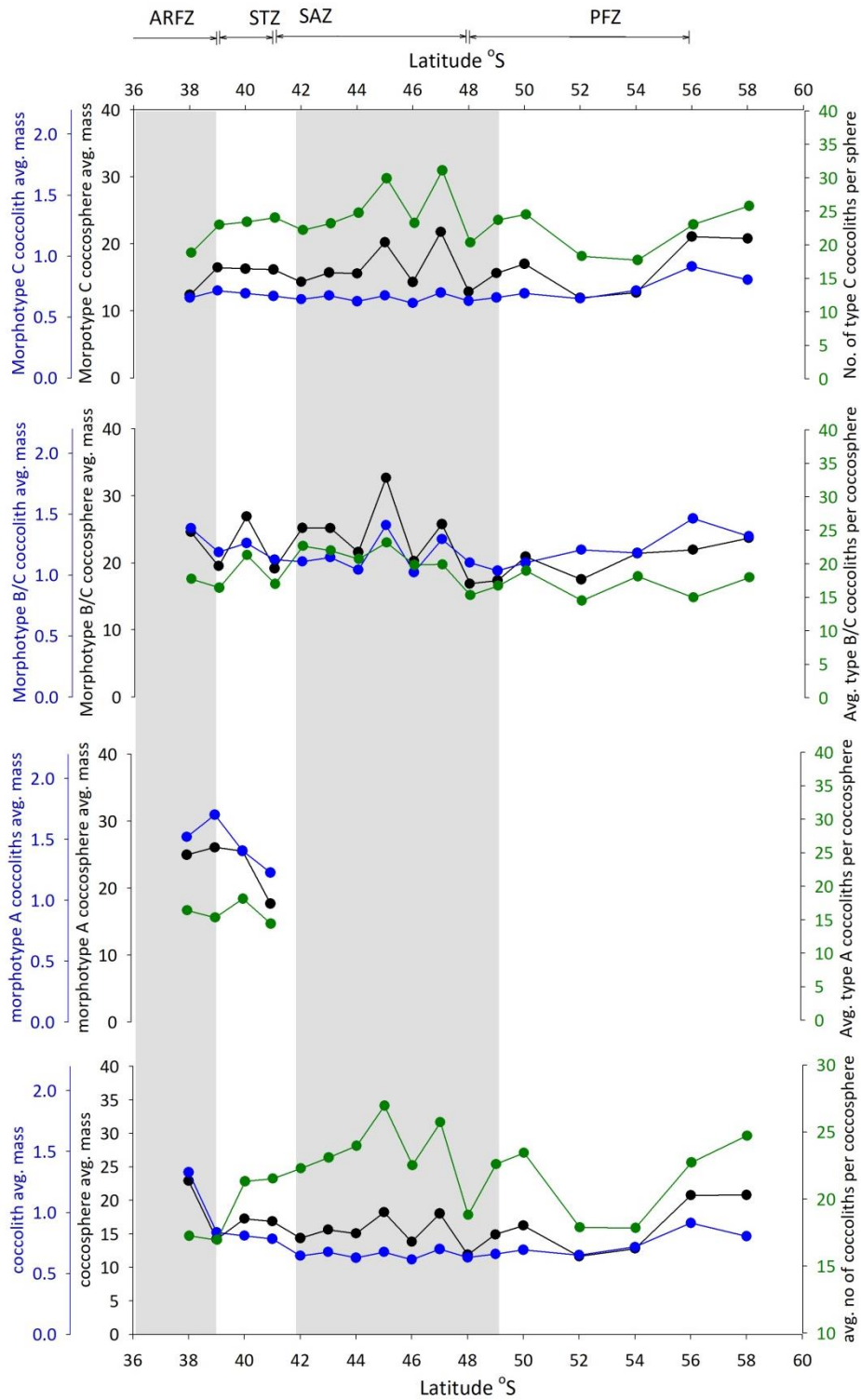


Fig. 6. *Emiliana huxleyi* coccolith and coccosphere mass, and number of coccoliths per coccosphere documented at 48°E transect.

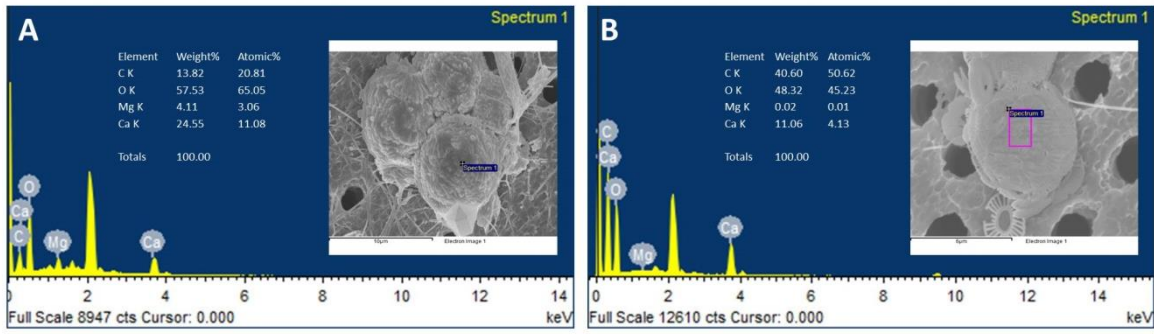


Fig. 7. Energy dispersive spectrometry analysis of (A) *E. huxleyi* overcalcified specimens indicating presence of Mg, and (B) regular coccosphere of *E. huxleyi* morphotype A.

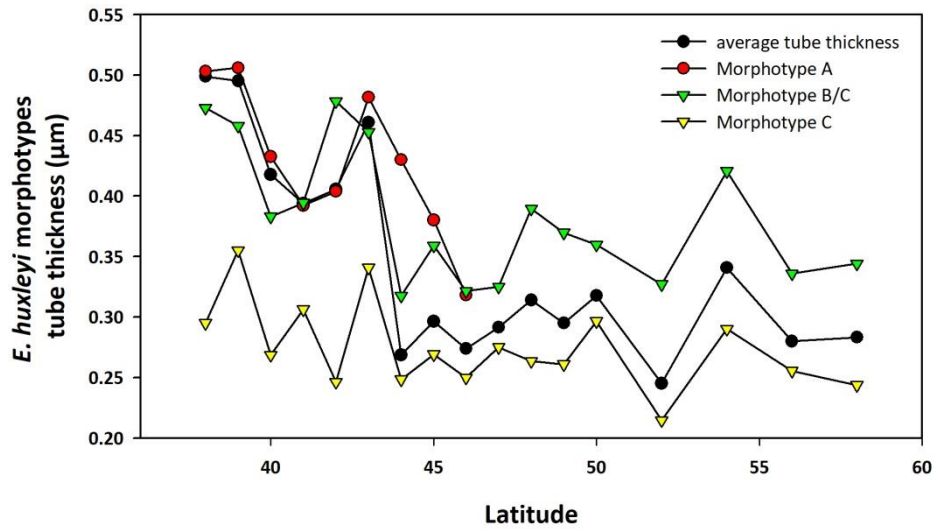


Fig. 8. Average *E. huxleyi* tube thickness and morphotypes A, B/C, and C tube thickness.

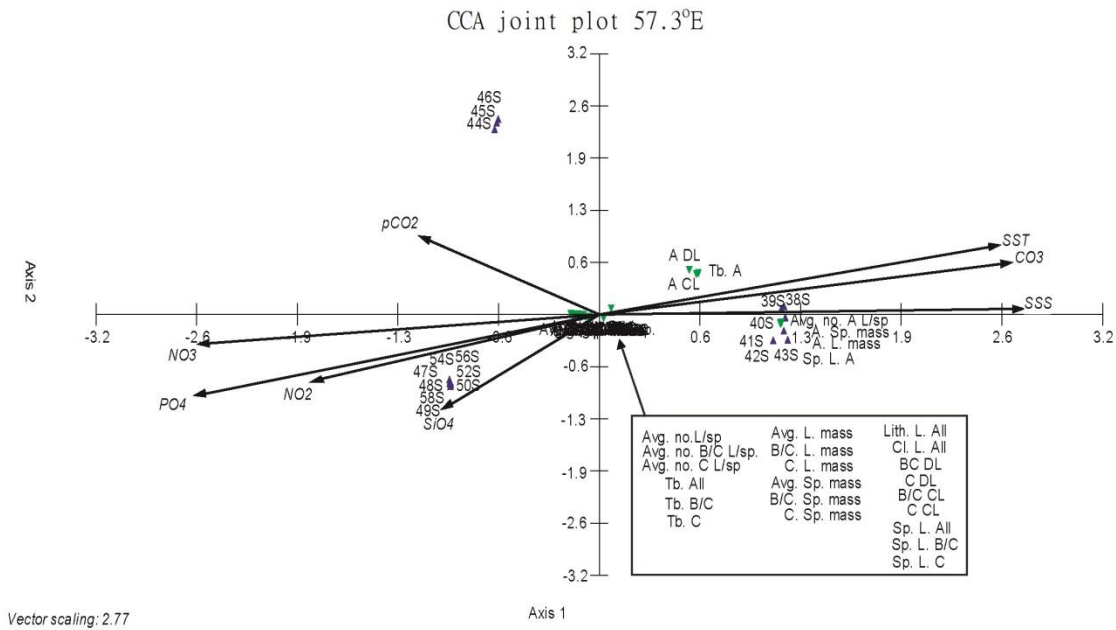


Fig. 9(a) CCA biplots showing the correlation between *Emiliana huxleyi* morphotype morphologies and environmental factors (arrows) in the 57.3°E transects. The details of codes are given in Table 3.

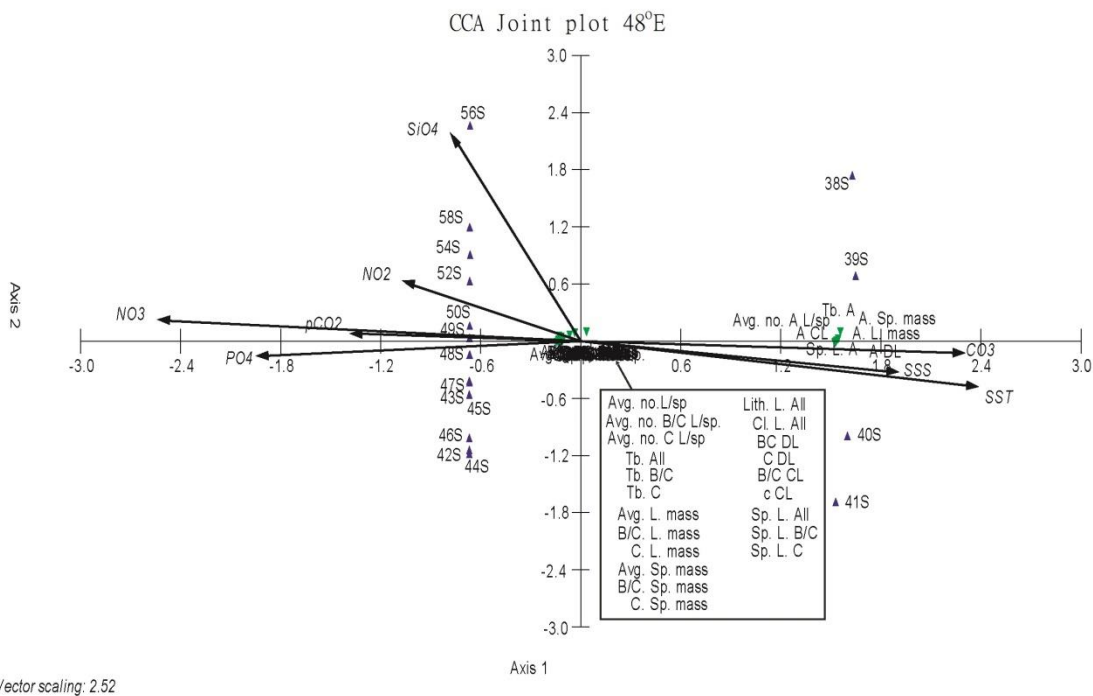


Fig. 9(b) CCA biplots showing the correlation between *Emiliana huxleyi* morphotype morphologies and environmental factors (arrows) in the 57.3°E transects. The details of codes are given in Table 3.

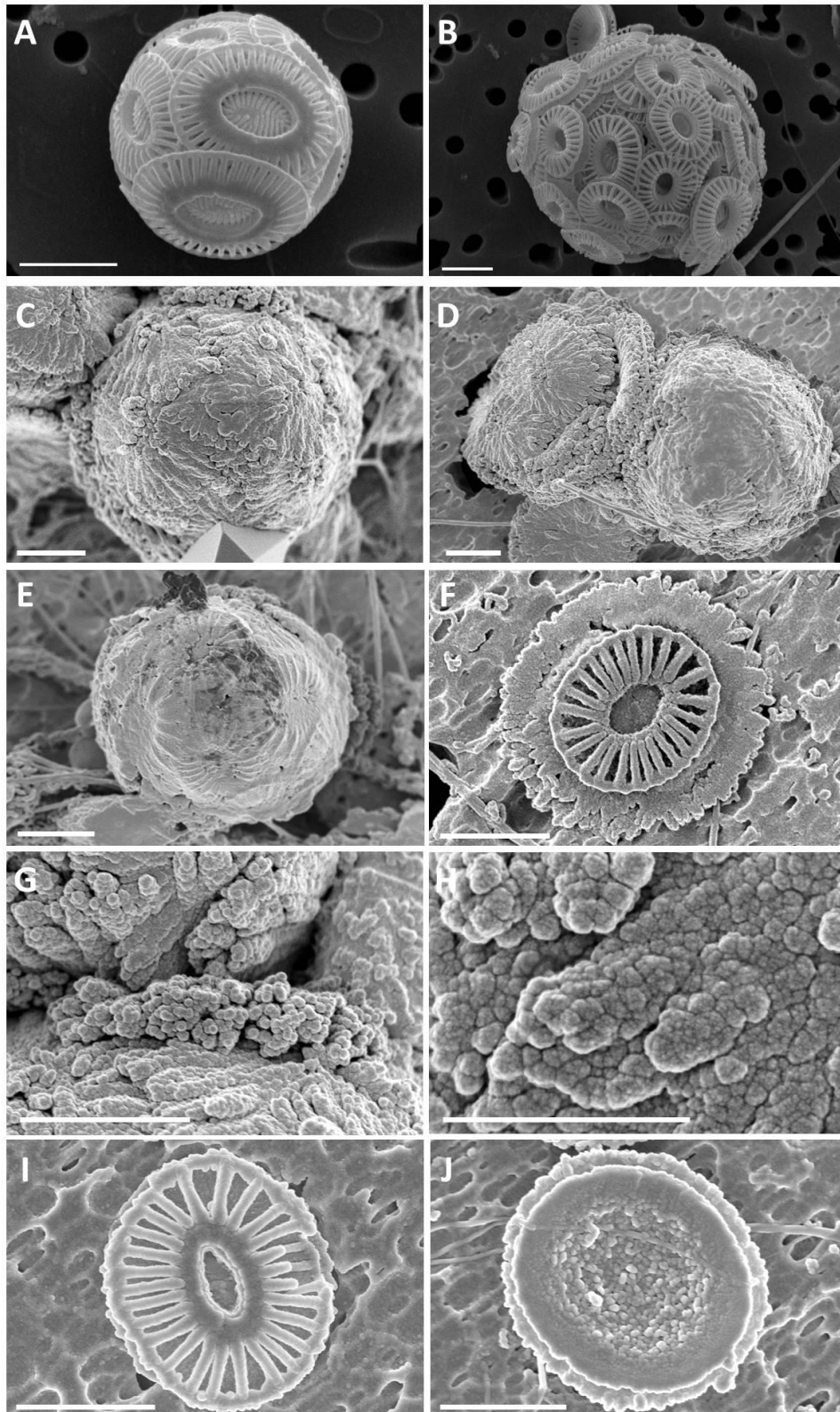


Plate. 1. (A) *E. huxleyi* morphotype A regular coccosphere (40°S, 57.3°E); (B) *E. huxleyi* morphotype C coccosphere (46°S, 57.3°E); (C-G) Overcalcified *Emiliana huxleyi* coccospheres; (H) overcalcified coccolith proximal shield; (I) Anterior view of overcalcified *E. huxleyi* coccolith; (J) posterior view of *E. huxleyi* overcalcified coccolith. [scale- A-G, I-J= 2 μ m; H-1 μ m].

Table 1. Sample details, physico-chemical parameters recorded/measured, and the total number of coccoliths and coccospheres used to carry out morphometric measurements

Latitude (°S)	Longitude (°E)	Collection date	Temperature (°C)	Salinity	NO3	NO2	PO4	SiO4	CO ₃ ²⁻	pCO ₂	Number of coccoliths measured	Numbers of coccospheres measured
38	57.3	31-01-2010	20	35.51	1.22	0.14	0.53	4.77	277	213	143	51
39	57.3	31-01-2010	18	35.31	2.16	0.00	0.13	6.84	270	196	118	54
40	57.3	01-02-2010	17.5	35.33	1.42	0.16	0.27	5.14	282	214	110	52
41	57.3	01-02-2010	16.5	35.43	4.67	0.18	0.71	5.33	265	189	120	53
42	57.3	02-02-2010	16	35.4	1.73	0.10	0.27	0.69	267	190	122	47
43	57.3	02-02-2010	16	35.45	1.51	0.02	0.27	4.01	270	195	118	51
44	57.3	03-02-2010	12	33.97	11.39	0.10	1.11	2.70	227	200	106	49
45	57.3	04-02-2010	11	33.79	12.79	0.12	0.71	4.14	202	263	126	51
46	57.3	05-02-2010	10.5	33.82	16.66	0.23	1.20	2.32	178	335	122	51
47	57.3	05-02-2010	10.5	33.76	13.80	0.27	1.82	3.58	198	262	106	49
48	57.3	06-02-2010	8	33.72	10.91	0.12	1.78	3.51	170	291	122	51
49	57.3	07-02-2010	7	33.69	16.35	0.27	1.82	3.58	141	290	125	50
50	57.3	07-02-2010	5	33.78	19.82	0.35	1.74	4.77	145	281	120	51
52	57.3	08-02-2010	4.5	33.83	29.32	0.21	1.74	14.55	158	270	122	52
54	57.3	09-02-2010	3.5	33.86	20.36	0.21	2.00	7.40	169	242	121	56
56	57.3	11-02-2010	2.5	33.35	20.99	0.21	1.51	20.51	138	350	118	55
58	57.3	12-02-2010	2	32.54	15.65	0.21	2.18	22.83	125	261	119	47
58	49.37	23-02-2010	2.5	33.81	21.26	0.31	2.80	13.36	115	321	122	50
56	48.31	23-02-2010	2.5	32.54	20.05	0.25	1.51	18.82	110	350	114	50
54	48	24-02-2010	4	33.73	19.07	0.35	1.74	11.16	119	394	127	52
52	48	25-02-2010	4.5	33.74	19.30	0.35	1.29	6.27	134	325	116	48
50	48	26-02-2010	5.5	32.51	17.47	0.18	1.56	4.08	150	280	119	50
49	48	26-02-2010	5.5	32.26	19.14	0.20	1.29	4.14	148	266	124	50

48	48	27-02-2010	6	32.33	18.75	0.16	1.51	4.08	137	328	127	49
47	48	27-02-2010	6	33.56	20.18	0.20	1.60	5.64	146	293	122	52
46	47.11	28-02-2010	8.5	33.77	16.71	0.12	1.25	3.64	193	246	124	50
45	47.54	01-03-2010	7	32.45	18.49	0.23	1.87	1.69	139	339	124	50
44	48	01-03-2010	8.5	33.63	16.68	0.18	2.00	1.76	152	323	127	54
43	48	02-03-2010	8.5	32.8	20.62	0.29	1.25	5.02	143	343	119	53
42	48.34	02-03-2010	10	33.57	17.48	0.27	1.07	2.38	156	315	125	62
41	49.36	03-03-2010	13	34.09	9.28	0.21	1.11	2.20	182	308	131	51
40	50.2	03-03-2020	16	34.78	4.55	0.12	0.93	2.51	265	237	121	55
39	50.57	04-03-2010	16	35.1	2.63	0.25	0.13	3.51	241	258	116	54
38	51.21	04-03-2010	18.5	33.81	7.39	0.10	0.31	5.71	278	227	121	50

Table 2. (1) *E. huxleyi* morphotype definitions adopted in this study and (2) size range of coccoliths and coccospheres measured

<i>E. huxleyi</i> morphotype	Morphological characteristics	Coccolith								Coccosphere			
		DL	DW	CL	CW	Elements	collar thickness/length	total coccolith area	Central area	length	width	area	coccoliths per sphere
<i>E. huxleyi</i> (all together)		2.62-3.27; avg-2.86	2.22-2.77; avg-2.46	0.99-1.54; avg-1.15	0.59-0.98; avg-0.70	22-32; avg-25	0.23-0.54; avg-0.32	4.59-7.11; avg-5.55	0.46-1.19; avg-0.64	4.88-7.63; avg-6.00	4.63-6.97; avg-5.65	17.94-13.12; avg-27.48	12-32; avg-21
<i>E. huxleyi</i> morphotype A	Heavily calcified warm water type, robust distal shield elements	2.76-3.28; avg-3.05	2.41-2.75; avg-2.59	1.02-1.55; avg-1.27	0.59-0.99; avg-0.77	26-32; avg-28	0.32-0.58; avg-0.45	5.26-7.07; avg-6.21	0.48-1.20; avg-0.78	5.20-5.99; avg-5.57	5-5.67; avg-5.38	20.74-26.63; avg-23.72	12-22; avg-16
<i>E. huxleyi</i> morphotype B	Delicate, long sized coccoliths, central area irregular laths, central area open or curved	3.39-4.47; avg-3.93	2.95-4.05; avg-3.36	1.41-1.82; avg-1.61	0.92-1.99; avg-1.16	30-35; avg-32.8	0.29-0.59; avg-0.42	7.85-14.22; avg-10.48	1.02-2.48; avg-1.47				
<i>E. huxleyi</i> morphotype B/C	Medium sized coccoliths, Delicate distal shield elements, central area open or covered	2.93-3.71; avg-3.13	2.51-3.22; avg-2.70	1.12-1.50; avg-1.24	0.66-0.97; avg-0.76	26-32; avg-27	0.25-0.52; avg-0.36	5.82-9.37; avg-6.66	0.59-1.14; avg-0.75	4.71-7.63; avg-6.12	4.67-7.06; avg-5.71	16.97-40.34; avg-28.07	12-24; avg-18
<i>E. huxleyi</i> morphotype C	small sized coccoliths, Distal shield elements delicate, central area open or covered	2.44-2.83; avg-2.57	2.06-2.47; avg-2.22	0.96-1.17; avg-1.02	0.54-0.72; avg-0.62	20-25; avg-22	0.21-0.35; avg-0.26	3.95-5.47; avg-4.49	0.41-0.65; avg-0.50	4.85-8.17; avg-6.14	4.60-8.16; avg-5.79	17.72-52.38; avg-28.89	16-36; avg-24

Table 3. CCA codes and description of the codes

CCA code	Description
Sp. L. All	<i>E. huxleyi</i> coccospheres mean length
Sp. L. A	<i>E. huxleyi</i> morphotype A coccosphere length
Sp. L. B/C	<i>E. huxleyi</i> morphotype B/C coccosphere length
Sp. L. C	<i>E. huxleyi</i> morphotype C coccosphere length
Lith. L. All	<i>E. huxleyi</i> coccoliths DL
A DL	<i>E. huxleyi</i> morphotype A coccolith DL
BC DL	<i>E. huxleyi</i> morphotype B/C coccolith DL
c DL	<i>E. huxleyi</i> morphotype C coccolith DL
Cl. L. All	<i>E. huxleyi</i> coccoliths CL
A CL	<i>E. huxleyi</i> morphotype A coccolith CL
B/C CL	<i>E. huxleyi</i> morphotype B/C coccolith CL
C CL	<i>E. huxleyi</i> morphotype C coccolith CL
Tb. All	<i>E. huxleyi</i> tube size
Tb. A	<i>E. huxleyi</i> morphotype A tube size
Tb. B/C	<i>E. huxleyi</i> morphotype B/C tube size
Tb. C	<i>E. huxleyi</i> morphotype C tube size
A. L. mass	<i>E. huxleyi</i> morphotype A coccolith mass
A. Sp. mass	<i>E. huxleyi</i> morphotype A coccosphere mass
B/C. L. mass	<i>E. huxleyi</i> morphotype B/C coccolith mass
B/C. Sp. Mass	<i>E. huxleyi</i> morphotype B/C coccosphere mass
C. L. mass	<i>E. huxleyi</i> morphotype C coccolith mass
C. Sp. Mass	<i>E. huxleyi</i> morphotype C coccosphere mass
Avg. L. mass	<i>E. huxleyi</i> coccolith mass
Avg. Sp. Mass	<i>E. huxleyi</i> coccosphere mass
Avg. no.L/sp	Number of coccoliths on a coccosphere
Avg. no. A L/sp	Number of coccoliths on a <i>E. huxleyi</i> morphotype A coccosphere
Avg. no. B/C L/sp.	Number of coccoliths on a <i>E. huxleyi</i> morphotype B/C coccosphere
Avg. no. C L/sp	Number of coccoliths on a <i>E. huxleyi</i> morphotype C coccosphere